Preliminary results based on geochemical sedimentary constraints on the hydrocarbon potential and depositional environment of a Messinian sub-salt mixed siliciclastic-carbonate succession onshore Crete (Plouti section, eastern Mediterranean)

George Kontakiotis, Vasileios Karakitsios, Jean-Jacques Cornée, Pierre Moissette, Stergios D Zarkogiannis, Nikolaos Pasadakis, Efterpi Koskeridou, Emmanouil Manoutsoglou, Hara Drinia, Assimina Antonarakou

Preliminary results based on geochemical sedimentary constraints on the hydrocarbon potential and depositional environment of a Messinian sub- salt mixed siliciclastic- carbonate succession onshore Crete (Plouti section, eastern Mediterranean)

George Kontakiotis[1] · Vasileios Karakitsios[1] · Jean- Jacques Cornée[2] · Pierre Moissette[1,3] · Stergios D. Zarkogiannis[1] · Nikolaos Pasadakis[4] · Efterpi Koskeridou[1] · Emmanouil Manoutsoglou[4] · Hara Drinia[1] · Assimina Antonarakou[1]

Abstract
This study details new geochemical analysis from an outcrop in Crete to improve understanding of the hydrocarbon potential of the southern margin of the Hellenic Arc along the continental convergent zone of the central Mediterranean Ridge. Seventeen samples were collected from the Late Miocene sub-salt sedimentary succession of Plouti section in central Crete and were studied in terms of their organic geochemical features using Rock–Eval VI pyrolysis. Results of this investigation revealed intervals with sufficient organic material of good enough quality and quantity to be considered as potential source rocks. The obtained data generally present poor to fair and/or good in some cases hydrocarbon generation potential. The TOC values range from 0.03 to 1.99%, with an average fair (2.1 mg HC/g rock) hydrocarbon potential. A Type III kerogen was identified, indicating a terrestrial origin organic matter. T_{max} and Production Index values suggest that the most promising parts of the section (organic-rich sediments) are immature with respect to oil generation and have not experienced high temperature during burial. Overall, the present study offers the opportunity to advance our understanding on the hydrocarbon potential onshore Crete and further investigate hydrocarbon prospectivity in the adjoining area, and particularly, the Greek part of the Mediterranean Ridge, a region with crucial economic and strategic importance.

Keywords Messinian Salinity Crisis (MSC) · Source-rocks · Sedimentary basin dynamics · Hydrocarbon potential · Kerogen type · Thermal maturity

Introduction

The exploration of accretionary prisms around the world (e.g., Barbados, Makran, Irrawaddy-Andaman, West Timor Through) has led to the discovery of substantial petroleum reserves (Dolan et al. 2004; Wandrey 2006; Escalona et al. 2008; Persad 2008; Jones et al. 2011; Klein et al. 2011). In the eastern Mediterranean, a large number of accretionary prism complexes, characterized by the fastest rates of increase in the world (Kopf et al. 2003), are encountered within the Mediterranean Ridge (MR) (Mann et al. 2003; Foscolos et al. 2012). This structure results from

the subduction of the African plate beneath the European plate (Olivet et al. 1982; Reillinger et al. 1997; Kreemer and Chamot-Rooke 2004) (Fig. 1). Hydrocarbon potential in this region, particularly along the subduction zone and collisional

margins, has been of long-standing academic and industrial interest (Zelilidis et al. 2003; Samuel et al. 2009; Bruneton et

al. 2011; Maravelis et al. 2012; Pantopoulos et al. 2013; Tsirambides 2015). However, recent discoveries have significantly altered the energy outlook in the region, with interest of the authorities and petroleum industry spurring additional exploration activities along the MR. The entire basin is increasingly becoming an exploration hotspot with both onshore and offshore frontier areas with potential for significant conventional and/or unconventional (shale gas and coal bed methane) hydrocarbon resources.

Fig. 1 Geodynamic map of the Eastern Mediterranean region showing the position of the main structures (e.g., thrust front, subduction zones) and the location of the study area (white dashed inset corresponding to Fig. 2). Red dots correspond to hydrocarbon fields along the

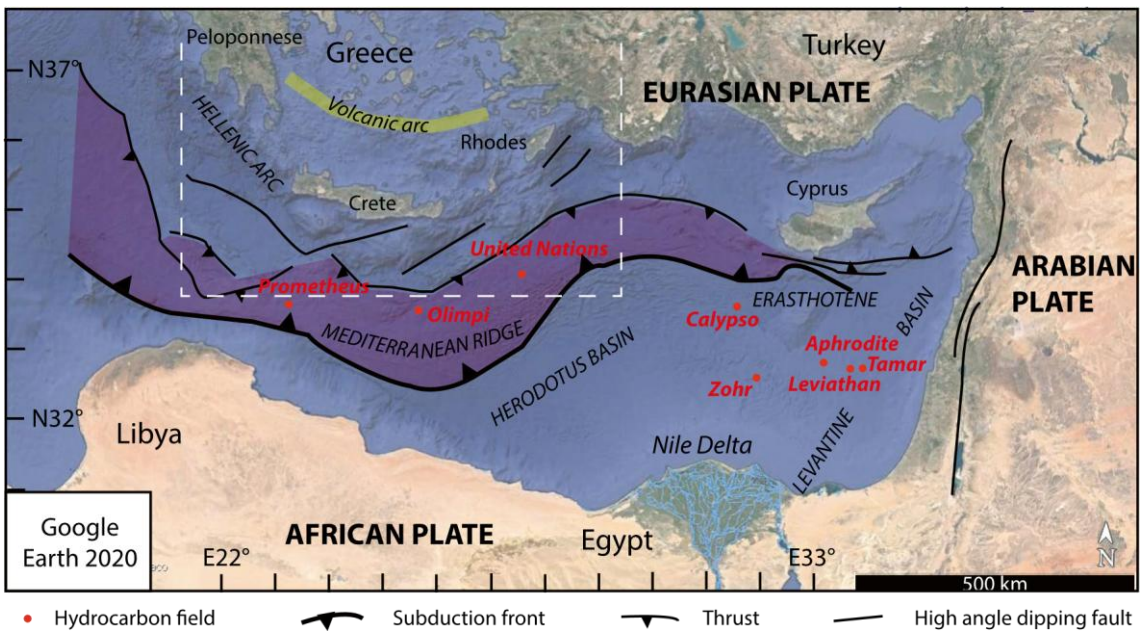

Mediterranean Ridge (purple highlighted area) and offshore Herodotus and Levantine basins within the eastern Mediterranean Sea

Proven hydrocarbon reserves have been reported in the surrounding region (e.g., Levantine basin), while areas meriting further exploration (e.g., Herodotus basin, offshore Crete) have been also highlighted (Gardosh and Druckman 2006; Roberts and Peace 2007; Semb 2009; Foscolos et al. 2012; Elia et al. 2013; Maravelis et al. 2015a, b). The latter, particularly lies partly in the Greek Exclusive Economic Zone (EEZ) and appears to have significant oil/gas potential, including probable large stratigraphic traps and working petroleum systems (Bruneton et al. 2011; Maravelis and Zelilidis 2011; Maravelis et al. 2012). Direct hydrocarbon evidence of thermogenic origin, such as active mud volcanoes, pock-marks, and pipenecks, which emit methane (gas) hydrates, have been also documented (Montadert and Nikolaides 2007; Lykousis et al. 2009; Krois et al. 2010; Pape et al. 2010; Foscolos et al. 2012; Bohrmann et al. 2014; Bertoni et al. 2017; Tamborrino et al. 2019), thus enhancing the future prospectivity of the MR. Particularly, south of Crete, the existence of Olimpi, Prometheus, and United Nations mud volcano fields with many active mud volcanoes (Cita et al. 1981; Camerlenghi et al. 1992; Chaumillon et al. 1996; Limonov et al. 1996; Cronin et al. 1997; Huguen et al. 2004, 2006;

Loncke et al. 2004; Haese et al. 2006; Praeg et al. 2007, 2011; Maravelis et al. 2015b) highlights the extent of Mediterranean gas hydrate areas (Fig. 1). Moreover, several recent large natural gas field discoveries in the offshore Levantine and Herodotus basins (Needham et al. 2013; Ratner 2016; Grohmann et al. 2018, 2019) make the eastern Mediterranean one of the most promising frontier basins of the world. These new fields comprise mainly natural gas of biogenic origin and are located in either Miocene clastic turbidites (e.g., Tamar and Leviathan-Israel, Aphrodite-Cyprus; Montadert et al. 2014; Bou Daher et al. 2016) or in Mesozoic shallow marine carbonate buildups (ZohrEgypt, Calypso-Cyprus; Schenk et al. 2010; Bertello et al. 2016; Esestime et al. 2016) (Fig. 1). However, in the offshore regions the characterization of potential source rocks is not a simple task, since almost no public well data and core samples are available. In this case, source rock properties and distribution have to be deduced from seismic interpretation and nearby onshore observations (e.g., Vafidis et al. 2012). High-resolution seismic data provide sufficient thickness of the sedimentary column, alternating sealing units, as well as direct hydrocarbon indicators (e.g., bright spots, gas chimneys; Roberts and Peace 2007; Montadert et al. 2014).

Onshore studies have identified several candidate source rock deposits in the sedimentary succession of the eastern Mediterranean Sea (Karakitsios and Rigakis 1996, 2007; Karakitsios et al. 2001; Zelilidis et al. 2003, 2015, 2016; Karakitsios 2013; Moforis et al. 2013; Maravelis et al. 2014, 2015a, 2016, 2017; Zelilidis and Maravelis 2015; Tserolas et al. 2018, 2019; Bourli et al. 2019a, b; Grohmann et al. 2019; Leila et al. 2020) in terms of Mesozoic oil-prone and Cenozoic gas-prone source rocks. Oil production in the study area is generally present in the sub-salt pre-Messinian sequences, while post-Messinian deposits have shown prospects for biogenic gas and are relatively immature in respect to hydrocarbon generation. More explicitly, the Late Miocene hydrocarbon generation potential onshore Crete and surrounding region has been documented in central Crete (Panagopoulos et al. 2011; Pasadakis et al. 2012; Maravelis et al. 2016), Gavdos Island (Pyliotis et al. 2013), and Levantine basin in the south-easternmost sector of the Mediterranean basin (Gardosh and Druckman 2006; Roberts and Peace 2007; Semb 2009; Grohmann et al. 2019).

A great opportunity to advance our understanding on the hydrocarbon potential onshore Crete is offered by the Late Miocene sedimentary rocks on the Heraklion inland frontier basin, central Crete. In particular, the deposition of sub-salt sediments with source rock and/or reservoir potential is crucial, since the evaporites may potentially serve as seals and therefore hold large hydrocarbon columns. The main target of the present study is focused on the Messinian sub-salt sedimentary succession of the Plouti section. These rocks were investigated with respect to the quantity and quality of sedimentary organic matter, their Total Organic Carbon (TOC) content and source rock potential, thermal maturity, and the corresponding depositional environment. All this information is also used to assess the possible mechanisms of source rock deposition and petroleum systems onshore Crete, which may provide important prospect for the Neogene petroleum concern of the broader area of the eastern Mediterranean Sea.

Geological setting

Tectonostratigraphic framework

The eastern Mediterranean basin is a relic of the Neo-Tethys Ocean and evolved from successive prototype basins that developed as a result of extension-convergence tectonic cycles, which was controlled by the interplay of the African, Arabian and Eurasian plates (Robertson 1998; Gardosh et al. 2010; Robertson et al. 2012; Montadert et al. 2014; Gao et al. 2019). It covers a wide geographical region, with its southern part bounded by the Cyprus Island and Hellenic arcs, and its northern part comprising the forearc accretionary zone associated with the Alpine orogeny (Fig. 1).

The evolution of the eastern Mediterranean Sea began in the Late Permian, associated with the breakup of Pangaea into several large continental fragments (Gardosh et al. 2010; Robertson et al. 2012). It further developed during Jurassic-Triassic rifting phases which caused the disintegration of Gondwana and the evolution of the Neo-Tethys Ocean (Segev and Rybakov 2010; Hawie et al. 2013; Ghalayini et al. 2014) as well as the separation of distinct subbasins (e.g., Herodotus, Levant and Eratosthenes continental block; Ben-Avraham et al. 2006; Montadert et al. 2014). During the Late Cretaceous, the tectonic regime changed from extensional to compressional, following the collision of the African-Arabian with the Eurasian plate (Hawie et al. 2013; Montadert et al. 2014). Subsidence in the Oligocene created the

deep northern Levant basin, which was filled with thick sequences of coarse clastic sediments supplied by the Nile Delta (Steinberg et al. 2011; Macgregor 2012). Since the Middle Eocene, the shrinking Neo-Tethys Ocean became separated from the Indian Ocean in the east, with the final isolation of the eastern Mediterranean Sea in the early-middle Miocene (Robertson et al. 2012).

During the latest Miocene, the Mediterranean basin was cut off from the Atlantic Ocean resulting in the Messinian Salinity Crisis (MSC; Hsü et al. 1973; Krijgsman et al. 1999; Roveri et al. 2014). Throughout the entire basin, thick evaporites were deposited, while its eastern sector was exposed above sea-level and eroded (Robertson 1998). The re-establishment of open marine conditions took place during the basal Pliocene through a flooding event (Garcia-Castellanos et al. 2009) which resulted in the deposition of biogenic limestones (Trubi Formation; Langereis and Hilgen 1991; Hilgen and Krijgsman 1999; Hüsing et al. 2009; Kontakiotis et al. 2016) in the depocenters and/or clastic sediments in the shelf (e.g., Nile Delta) and slope areas (e.g., Herodotus and Levant basins; Gardosh and Druckman 2006; Frey-Martinez et al. 2007). At present, the region is dominated by the collision and continued convergence of the African and Eurasian plates, and related subduction, with the MR representing its accretionary wedge (Camerlenghi and Cita 1987; Reillinger et al. 1997; Robertson and Kopf 1998; Huguen et al. 2001; Kreemer and Chamot-Rooke 2004; Van Hinsbergen et al. 2005) (Fig. 2).

Neogene sedimentary environments of Heraklion basin

Today, Crete, as part of the Aegean micro-plate, is connected with the European continent (Meulenkamp et al. 1994). The island of Crete represents a prominent horst structure formed in the recent fore-arc of the still ongoing Hellenic subduction. The structure of Crete consists of a pile of nappes that contain rock units from various paleogeographic zones (Papanikolaou and Vassilakis 2010; Zachariasse et al. 2011). Particularly, its Neogene basins formed in response to extensional geodynamic processes in the Aegean region during the Middle Miocene (Fassoulas 2001) and show a high degree of similarity with regard to lithofacies and history of subsidence and inversion (Meulenkamp 1979). Subsidence occurred in complex half-graben systems in a variety of larger and smaller basins being separated by pronounced uplifted blocks composed of pre-Neogene sediments (e.g., limestones, sandstones, phyllites-quartzites, ophiolites; ten Veen and Postma 1999).

The present-day Heraklion basin is formed by a series of N-S trending half-grabens filled by clastics, carbonates

Fig. 2 Present-day geodynamic framework of the Hellenic Arc and approximate relative motion vector of the south Aegean in respect to stable Eurasia (Le Pichon et al. 1995; Mantovani et al. 2000; Sakellariou and Tsampouraki-Kraounaki 2019). The dashed black line corresponds to the Mediterranean Ridge accretionary complex. The circular arrows represent total rotation at the two ends of the Hellenic arc since 15 Ma, consistent with paleomagnetic observations (Kissel and Laj 1988). The red triangles show the Pleistocene to recent volcanism along the Hellenic volcanic arc, and the black star the regional location of the Plouti section in central Crete, within the eastern Mediterranean Sea

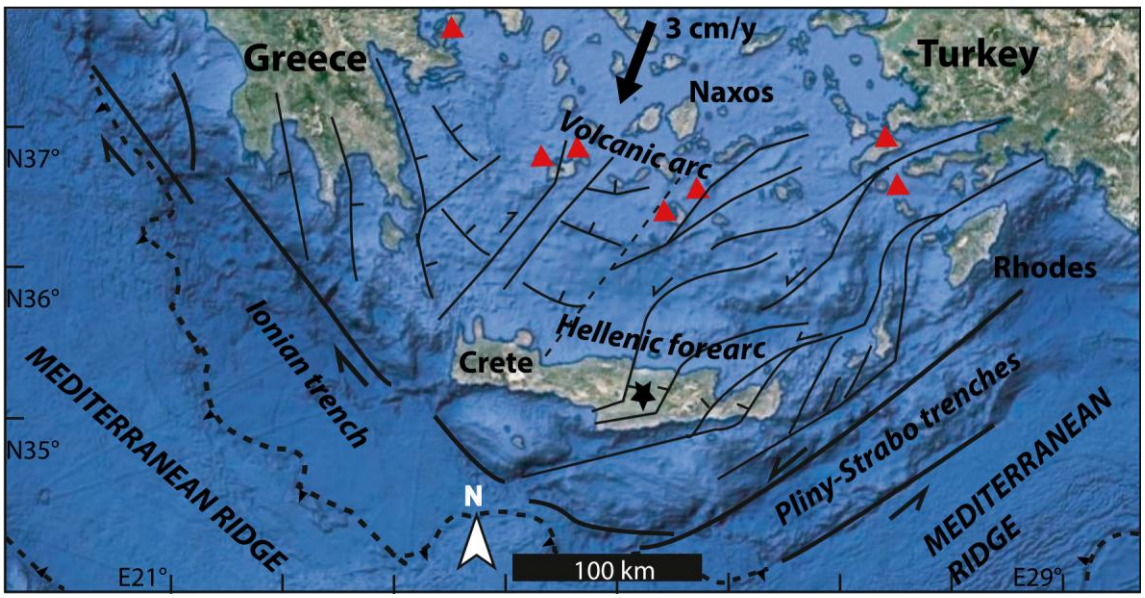

and evaporites of middle Miocene to Pliocene age (Meulenkamp 1979; Zachariasse et al. 2008, 2011). During this time interval, a sequence of different sedimentary environments from brackish lagoons to marginal and offshore marine settings have been documented in Crete (ten Veen and Postma 1999; Reuter et al. 2006; Drinia et al. 2008; Zachariasse et al. 2011; Moissette et al. 2018; Kontakiotis et al. 2019). Subsequent to a phase of non-marine and marginally marine sedimentation at the end of the Serravallian, the basin became a marine environment during the early Tortonian. Extensional tectonics during the late Tortonian triggered rotational uplift of blocks in positions distal to the basin margin and gave rise to pure offshore carbonate environments. Around the Tortonian-Messinian Transition, most shallow-water environments drowned during a pulse of relative basin subsidence and hinterland uplift. During the late Miocene, these blocks formed islands undergoing erosion and supplying the basin with siliciclastic fluvial, brackish, and marine sediments (Kontopoulos et al. 1996; Reuter et al. 2006; Zachariasse et al. 2008, 2011; Moissette et al. 2018).

Lithostratigraphy of the Plouti section

The Plouti Sect. (35° 05′ 44.1″ N, 24° 56′ 53.5″ E) corresponds to the uppermost part of the Messinian Vrysses Group (Fig. 3) and to the upper Messinian Lower Evaporites unit which is 50- to 60-m thick (Zachariasse et al. 2008). The uppermost part of the Vrysses Group in the Plouti area comprises 10-m thick alternations of silty marls, limestones and sandstones, topped by an erosional unconformity below the first gypsum beds (Fig. 4a,c), that are related to the Primary Lower Gypsum (PLG) and reflect the first phase of the MSC (p-ev1 at 5.97–5.60 Ma; CIESM 2008; Roveri et al. 2008; Manzi et al. 2012, 2013). The interval studied here concerns the last 10 m of sediments below the first gypsum bed. This sedimentary sequence mostly consists of fossiliferous silty clays and sandy limestones with some intercalations of diatomaceous marls enriched in tree leaves and siliceous sponge spicules (Fig. 4). The siliciclastic character of the above sediments further confirms their deposition during stressed (e.g., reduction of ocean connections, salinity fluctuations; Esteban 1979; Martín and Braga 1994; Moissette et al. 2010; Leila et al. 2020) conditions of the Terminal Carbonate Complex (TCC; Roveri et al. 2009; Bourillot et al. 2010) and also records the onset of the MSC (Cornée et al. 2004). Along the section, abundant traces of sulfur are displayed (Fig. 4b), indicating that these sediments were deposited in lagoonal restricted paleoenvironments. The occurrence of dominant sponges, associated with poorly diversified and scarce benthic fauna, also reveal oxygen depleted conditions. However, the presence throughout, but mostly at the base of the section (black shales), even if scarce, of planktonic and benthic foraminifera, bryozoans, and echinoids, points to marine influences. At the top of the studied interval, there is

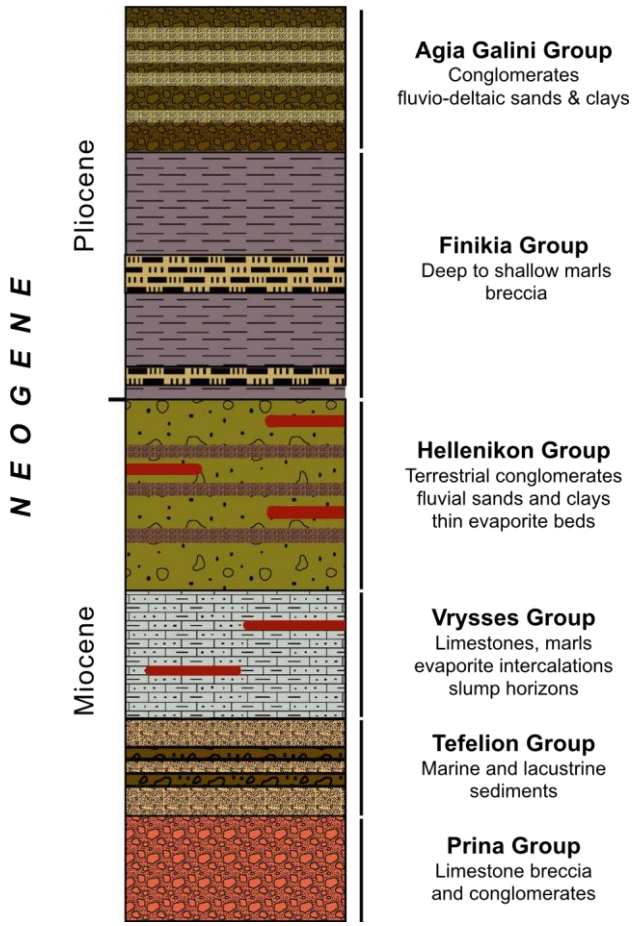

Fig. 3 General stratigraphy of Neogene sedimentary sequence in Crete Island with the six lithostratigraphic groups of Meulenkamp (1979) (modified after Zelilidis et al. 2016)

evidence of breccias composed of gypsum- and non-fossiliferous limestone clasts floating in a siltic to arenitic calcareous matrix (Fig. 4). Further up-sequence, an upward exposed alternation of non-fossiliferous clayey to silty marls with laminated gypsum beds, interpreted as shallow-water gypsum turbidites (Zachariasse et al. 2008), and fine-to coarsegrained terrigenous clastics forms a thick sedimentary package, equivalent to the Resedimented Lower Gypsum unit (RLG; Manzi et al. 2011) of the second phase of the MSC (p-ev2 at 5.60–5.55 Ma; Hilgen et al. 2007; CIESM 2008; Roveri et al. 2014).

Materials and methods

Sample collection and preparation

Seventeen rock samples, which were suspected to be rich in organic matter, were collected from the study outcrop on the island of Crete for geochemical analysis (Rock–Eval and detailed characterization of the contained organic matter). The selected samples were collected from the pre-evaporitic sedimentary succession of the Plouti section. Weathering is always a factor of concern for organic geochemical studies of outcrop samples and all analyzed samples were thus taken from at least 30 cm below the outcrop surface to minimize these effects. The fresh samples were immediately placed into plastic sample bags, secured with a zip tie, labelled with a unique sample number (PLO1-PLO17) and were taken to the laboratory for analyses. The experimental analytical work was carried out in the ‘‘Hydrocarbons Chemistry and

Technology Laboratory" of the Technical University of Crete. The samples were powdered and sieved through a 60-mesh (250 μm) sieve and analyzed using Rock–Eval (RE) pyrolysis technique with a Rock–Eval VI (Delsi Inc.) analyzer under standard conditions (e.g., programmed heating of ~ 100 mg of pulverized rock samples in an helium atmosphere in a special oven, and the hydrocarbons generated are monitored as a function of temperature; Espitalié et al. 1977, 1985; Peters 1986; Lafargue et al. 1998; Behar et al. 2001).

RE pyrolysis- derived parameters and interpretive guidelines

Source rock potential has been evaluated on the basis of three fundamental attributes: quantity, quality and maturity of the organic matter. Through this process, several important Rock–Eval derived parameters that are generated from the analysis are: S_1 (free hydrocarbons present within the sample released during the pyrolysis stage; mg HC/g rock), S_2 (heavier hydrocarbons released due to pyrolytic breakdown of kerogen released during the pyrolysis stage; mg HC/g rock), T_{max} (temperature at which maximum amount of pyrolyzate is cracked under the S_2 peak of Rock–Eval; °C), S_3 (CO_2 released from oxygenated compounds during the pyrolysis stage; mg C O_2/g rock), pyrolyzable carbon (PC; calculated from S_1, S_2, and S_3 components), S_4 (residual carbon (RC) content of the sample; mg carbon/g rock), hydrocarbon potential (HP equal to S_1 + S_2, mg HC/g rock), and TOC (sum of PC and RC; wt%), from which S_1/TOC ratio can be calculated. The free hydrocarbons liberated under the S_1 peak could be indigenous (free or adsorbed gas/oil) and/or non-indigenous (migrated or contaminated) in nature (Hunt 1996). The heavier hydrocarbons generated under the S_2 peak indicates the remaining hydrocarbon generation capacity of the rock (Tyson 1995), and is used to infer the Van Krevelen Types of organic matter input by calculating hydrogen indices (e.g., HI; S_2 normalized to TOC, mg HC/g TOC). Similarly, the S_3 peak is used to calculate oxygen indices (e.g., OI; S_3 normalized to TOC, mg C O_2/g TOC; Espitalié et al. 1977). Both the HI (100*S_2/TOC mg HC/g Corg) and OI (100*S_3/TOC mg CO_2/g Corg) have been used to define the kerogen type present in the rocks (Tissot and

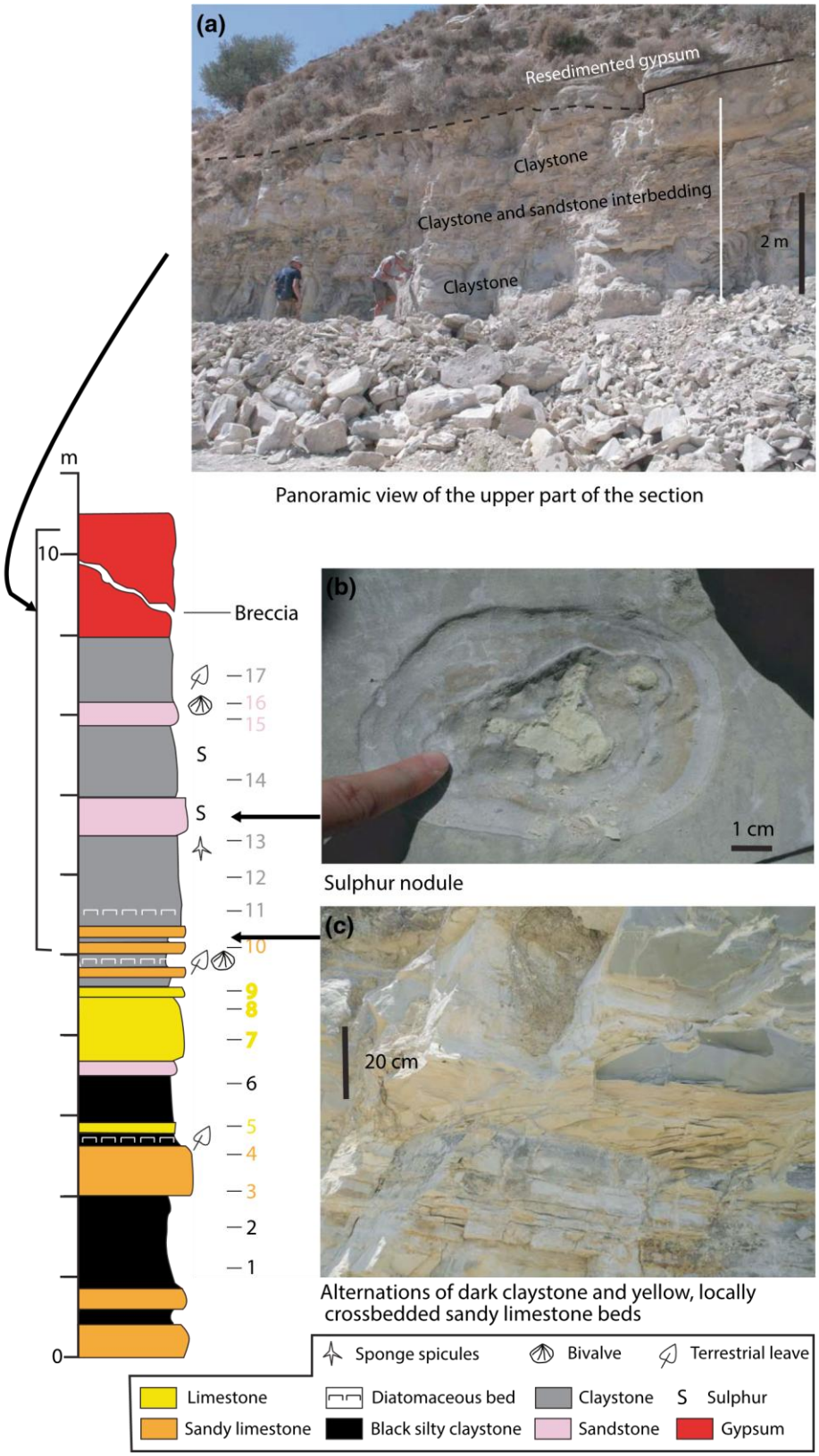

Fig. 4 Lithostratigraphic log and sedimentary facies characteristics of the Plouti section. To the right of the log are indicated the positions of the studied samples along with those of sponge spicules, bivalves, and terrestrial leaves identified in the different stratigraphic levels of the section. **a** Panoramic view of the upper part of the study section, **b** sulphur nodule, and **c** alternations of dark claystone and yellow, locally cross-bedded sandy limestone beds

Welte 1984; Tyson 1995; Hunt 1996) through the kerogen classifying diagram (Espitalié et al. 1977). Particularly, HI reflects the quality and quantity of pyrolyzable organic compounds, from S_2 relative to the TOC (mg HC/g TOC), while OI is related to the quantity of terrestrial organic matter. T_{max} is used as a maturity parameter for fossil organic matter

(Tissot and Welte 1984). Production Index (PI; $S_1/S_1 + S_2$) reveals the total amount of hydrocarbons ($S_1 + S_2$) that may be produced (Jones 1984). For the interpretation of the RE pyrolysis data, we refer to the specific guidelines of Tissot and Welte (1984), Peters (1986), Peters and Cassa (1994), Burwood et al. (1995), and Dymann et al. (1996). Geochemical parameters (e.g., HI, S_2/S_3) describing the type of hydrocarbons generated were also used as initially introduced by Peters (1986).

Results

Screening Plouti data

Bulk organic geochemical characteristics of the Messinian depositional sequence of Plouti section are summarized in Table 1, while the correlation of the RE results with lithology is further illustrated in Figs. 5, 6, and 7. TOC values range from 0.03 to 1.99%, with an average of 0.65%. Most of the analyzed samples show very low (< 0.5%) TOC contents; however, 6 samples (4 claystones and 2 limestones) present TOC values between 1 and 2% that can be classified as "Good Source Rock". S_1 values reflecting the presentday hydrocarbon generative capacity of kerogen in the rocks range from 0.01 to 0.70 HC/g rock. This may reflect the oxidation of the organic matter as is usually the case in late Miocene outcrop samples. The consistent low S_1 values further lead to relatively low production index values, ranging between $0.07 < PI < 0.21$. S_2 values are quite variable presenting either low (< 0.10 HC/g rock) or extremely high (> 3.0 HC/g rock) values, and this distribution is also evident for the hydrocarbon potential of the analyzed samples with the relevant HP values ranging between 0.03 and 7.57 mg HC/g rock. All studied samples reach a very narrow range of T_{max} values from 400 to 417 °C, indicative of their thermally immature character. HI and OI values vary between 57.53 and 417.56 HC/g TOC, and 61.45 and 1020.39 mg CO_2/g Corg, respectively.

Discussion

Definition of effective source rocks through TOC enrichment

There is a consensus that the TOC content, which is associated with free hydrocarbons and kerogen, can serve as a standard for evaluating the organic richness (quality) of source rocks. The lower threshold TOC limit for effective source rock is generally 0.5% (Hunt 1967, 1979, 1996; Tissot and Welte 1984). The Plouti TOC contents vary within the studied samples and range from 0.03% (PLO16) to 1.99% (PLO7). These values permit sample classification, in terms of their source rock potential, as mudstones with limited to good hydrocarbon generating potential. Samples PLO2, PLO6-PLO8, PLO12, PLO14, and PLO17 have merits for further consideration (0.5% < TOC < 2.0%). According to Zhao et al. (2015), the value of TOC corresponding to the beginning of the S_1/TOC value reduction is the base limit of TOC values for high-quality hydrocarbon source rocks. However, the application of this method to our data is minimized due to the small number of analyzed samples. Based on the above criteria, we follow the classification of Tissot and Welte (1984), where the minimum TOC value required characterizing a sample as at least an immature source rock is 0.5 wt%. Rocks containing < 0.5% TOC are considered to have negligible hydrocarbon source potential, while between 0.5 and 1.0% TOC indicates marginal potential, and > 1.0% TOC has substantial source potential.

Overall, the Plouti succession is classified as variable, mostly "poor" (10 samples; 58.8%) to "fair" (1 sample; 5.9%) and "good" (6 samples; 35.3%), according to TOC content (Table 1). Seven samples reached the standard for effective source rocks (TOC > 0.5%), with 5 of them belonging to black shales/claystones (black circles in Figs. 5, 6 and 7) and the rest to be classified as limestones (blue diamonds, respectively). Both sandstone samples (red triangles) display very low TOC content (< 0.1%; Figs. 5 and 6). All of them were immature (T_{max} < 435 °C), suggesting that these source rocks had not generated hydrocarbons in the study area. The average petroleum potential of 2.1 mg HC/g rock indicates a marginally "fair" source rock potential, which is in accordance with the average petroleum potential evaluated based on S_2 values (1.84 mg HC/g rock; Table 1).

Source rock potential

TOC alone is not a clear indicator of the hydrocarbon generation potential and thus, the carbon and hydrogen

Table 1 Geochemical indices obtained from the Rock–Eval VI analysis of the studied rock samples of the Plouti section

Sample ID	Lithology	T_{max} (°C)	S_1 (mg/g)	S_2 (mg/g)	S_3 (mg/g)	S_4 (mg/g)	TOC (%)	HI (mg HC/g TOC)	OI (mg CO_2/g TOC)	PI	S_2/S_3	S_1+S_2	S_1/TOC (mg HC/g TOC
PLO17	Claystone	405	0.23	2.83	1.02	8.18	1.07	265.05	95.36	0.07	2.78	3.06	0.21
PLO16	Sandstone		0.01	0.02	0.34	0.31	0.03	74.12	1020.39	0.29	0.07	0.03	0.30
PLO15	Sandstone		0.02	0.10	0.40	0.67	0.08	124.98	518.53	0.18	0.24	0.12	0.27
PLO14	Claystone	407	0.26	3.14	0.89	7.98	1.08	291.89	82.73	0.08	3.53	3.41	0.25
PLO13	Claystone		0.01	0.05	0.39	0.35	0.04	135.61	971.84	0.15	0.14	0.06	0.25
PLO12	Claystone	406	0.48	5.58	1.86	12.16	1.71	325.70	108.79	0.08	2.99	6.05	0.28
PLO11	Claystone	413	0.06	0.41	0.83	2.04	0.24	168.03	340.49	0.13	0.49	0.47	0.26
PLO10	Limestone		0.01	0.05	0.33	0.55	0.06	86.37	555.49	0.19	0.16	0.06	0.20
PLO9	Limestone		0.01	0.04	0.39	0.62	0.07	57.53	584.10	0.21	0.10	0.05	0.15
PLO8	Limestone	403	0.52	5.29	1.15	13.88	1.86	283.47	61.45	0.09	4.61	5.81	0.28
PLO7	Limestone	400	0.56	5.28	1.29	15.11	1.99	265.43	64.96	0.10	4.09	5.84	0.28
PLO6	Claystone	417	0.10	0.89	0.95	5.08	0.59	150.96	161.25	0.11	0.94	1.00	0.18
PLO5	Limestone	415	0.04	0.32	0.64	2.41	0.27	119.59	237.99	0.11	0.50	0.36	0.15
PLO4	Limestone	416	0.02	0.20	0.30	1.31	0.15	133.20	201.02	0.09	0.66	0.22	0.14
PLO3	Limestone		0.01	0.04	0.37	0.60	0.06	62.25	572.43	0.20	0.11	0.05	0.16
PLO2	Claystone	403	0.70	6.87	1.24	10.25	1.65	417.56	75.35	0.09	5.54	7.57	0.42
PLO1	Claystone		0.03	0.09	0.71	1.34	0.14	64.71	494.30	0.24	0.13	0.12	0.21

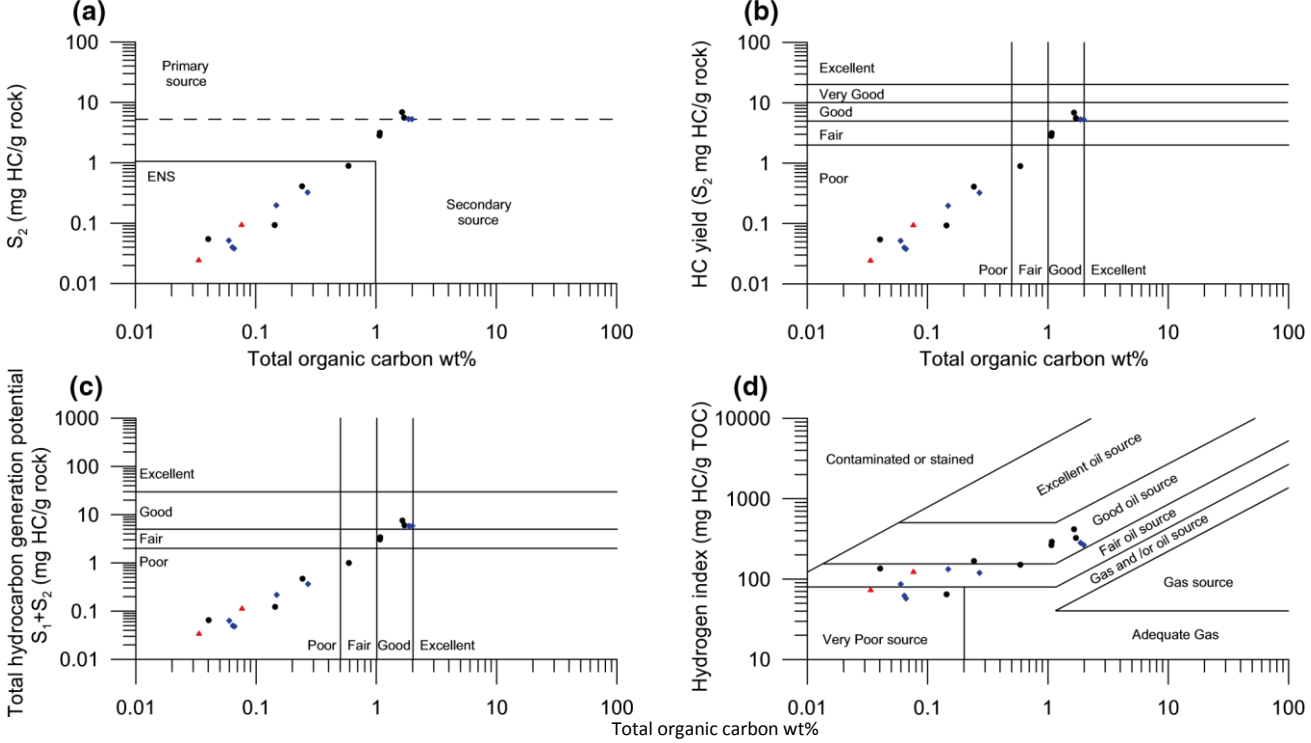

Fig. 5 Source rock appraisal of the examined samples from Plouti section based on: **a**, **b** cross-plots of S_2 versus total organic carbon, **c** total hydrocarbon generating potential versus total organic carbon

Total organic carbon wt%

classification diagram, **d** hydrogen index versus total organic carbon biplot. These plots indicate the presence of source rocks with poor to good hydrocarbon generating potential

contents of the organic matter are required (Dembicki 2009). The S_2 value that reflects the quantification of the amount of hydrocarbons formed during the thermal decomposition of the kerogen, integrated with TOC values can add constraints in the hydrocarbon generating potential of the source rocks. The S_2 values range from 0.02 mg HC/g rock (PLO16) to 6.87 mg HC/g rock (PLO2). The cross-plot of S_2 versus TOC classifies the studied sediments principally as secondary effective non-source rocks (ENS; S_2 < 1 mg HC/g rock), with the exception of 4 samples which are marginally classified as primary source rocks (S_2 > 5 mg HC/g rock). This plot portrays the occurrence of relatively lean source rocks with poor to good hydrocarbon generating potential (Fig. 5a). This is further supported by the hydrocarbon yield S_2 versus TOC crossplot of Burwood et al. (1995) which indicates that samples with higher S_2 values correspond to higher quality source rocks (Fig. 5b). The cross-plot showing the relationship of total generative hydrocarbon potential HP versus TOC demonstrates a variable distribution of the source rock potential. Although most of the samples suggest insignificant (HP < 2 mg HC/g rock) oil (but some gas) potential, two samples (black shales) were classified as moderately rich source rocks with fair (2 mg HC/g rock < HP < 5 mg HC/g rock) oil potential, and four other samples (two black shales and two limestones) classified as good (HP > 5 mg HC/g rock) source rock potential (Tissot and Welte 1984; Dymann et al. 1996) (Fig. 5c). The different source rock potential estimations could be partly explained by inert organic carbon within the TOC. A better rating of source rock potential is given by the cross-plot of HI versus TOC (Jackson et al. 1985), which shows a clear oil-prone source rock potential, with the majority of the samples almost equally distributed within the fair and good oil-prone windows (Fig. 5d). However, the integration of parameters such as chemistry, maturation status, and description of organic matter, is essential before a rock can be regarded as oil-prone.

Quality and type of organic matter

The type of organic matter contained in the source rocks was evaluated by the HI and the S_2/S_3 ratio (Peters 1986). Both these parameters indicate mainly the occurrence of gas and/ or oil + gas prone organic matter (Fig. 6a,b). The reported

HI values below 150 mg HC/g TOC indicate a potential source for generating gas (mainly type III kerogen), while the relevant values ranging between 150 and 300 mg/g contain

0.01 0.1 1 10 100

Total organic carbon wt% **(c)**

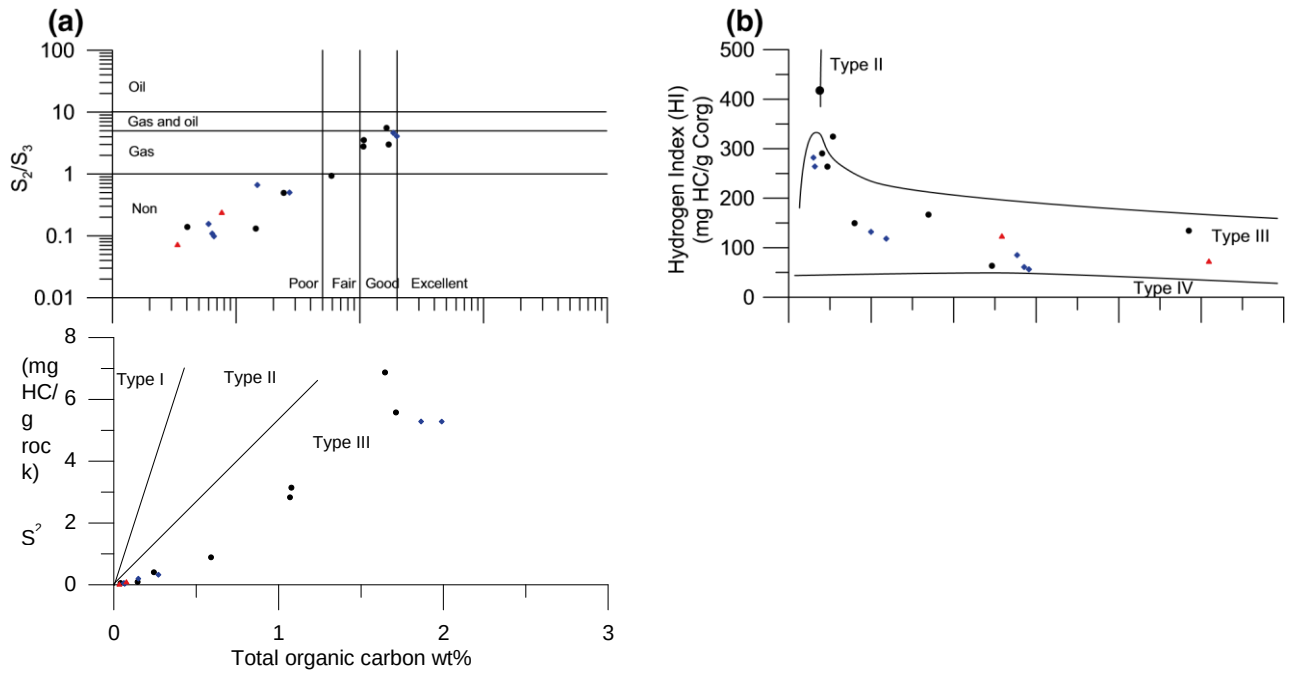

Fig. 6 Results of Rock–Eval VI pyrolysis plotted on: **a** S_2/S_3 versus total organic carbon, **b** hydrogen index versus oxygen index kerogen classification diagram, **c** S_2 versus total organic carbon classification

0 200 400 600 800 1000 1200

Oxygen Index (OI) ($mgCO_2g/Corg$)

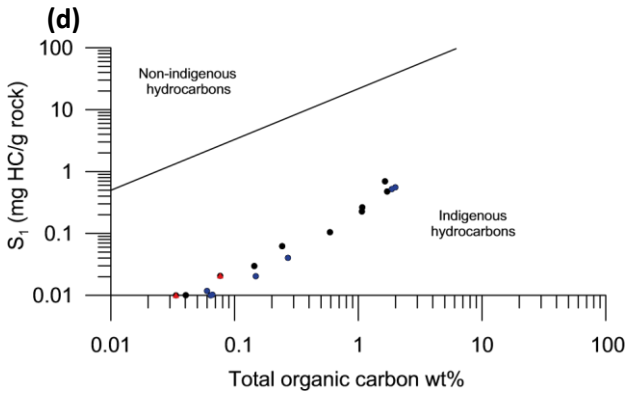

diagram, **d** plot of S_1 versus total organic carbon. These plots indicate the presence of nonproductive to gas-prone source rocks capable of generating autochthonous hydrocarbons

Fig. 7 Classification of kerogens and maturation status of the examined samples based on: **a** Hydrogen index versus T_{max} diagram, and **b** cross-plot of production index versus T_{max}. These diagrams portray co-existence of samples with oil and gas generating potential. The majority of the Plouti samples are immature with respect to oil generation and have not experienced very high temperatures during burial

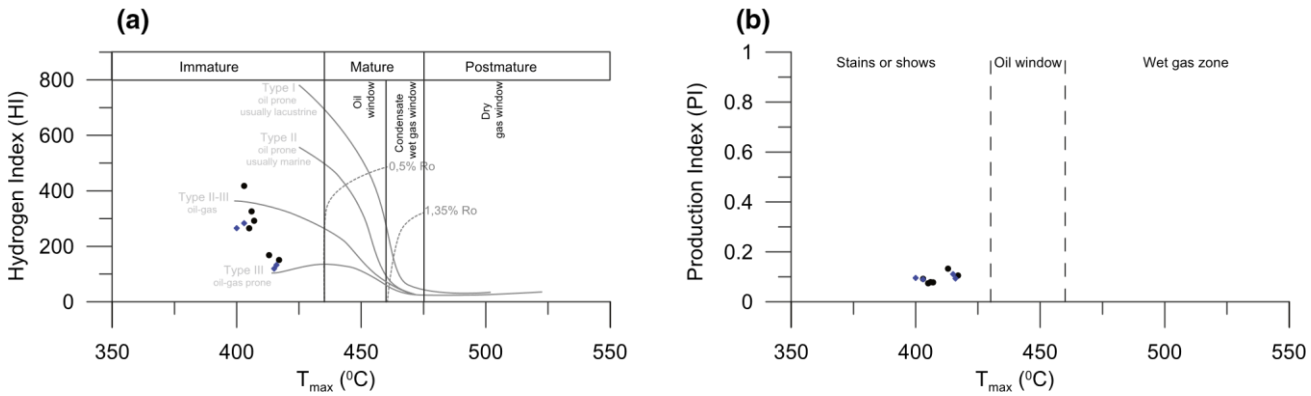

mostly type III kerogen, and therefore, are capable of generating mixed gas and oil (Fig. 6b). Only two samples (PLO2 and PLO12) present > 300 mg/g value, along with their high TOC content (1.65 and 1.71 wt%, respectively), suggesting the presence of a significant amount of oil-generative lipid materials possibly derived from autochthonous organic matter inputs under a reducing depositional environment. Their gaseous generation potential is further indicated using the S_2/S_3 scheme proposed by Peters (1986), which suggests the occurrence of gas-prone rocks ($1 < S_2/S_3 < 5$) (Fig. 6a). Additional characterization of the organic matter quality was made based on HI versus OI cross-plot (Fig. 6b; Peters and Cassa 1994). The application of the above classification scheme on the studied samples indicates the occurrence of type III kerogen that originated from terrestrial plant debris and/or aquatic organic matter, and was deposited in an oxidizing shelf environment. Supporting evidence for the dominance of type III kerogen in the examined samples comes from the S_2 versus TOC cross-plot (Fig. 6c; Tissot and Welte 1984). Although type III kerogen can be associated with aquatic organic matter in marine settings (Tissot et al. 1974), its prevalence in the studied sediments can be also related to transportation by fluvial processes (Vandenbroucke and Largeau 2007). Late Miocene runoff into the eastern

Mediterranean basin was at least three times greater than that of today (Gladstone et al. 2007), based on the cumulative effect of the African rivers in the south and the Paratethys freshwater supply in the north (Krijgsman et al. 2010; Moissette et al. 2010; Natalicchio et al. 2014; Karakitsios et al. 2013, 2017a, b; Van Baak et al. 2017; Vasiliev et al. 2019; Grothe et al. 2020). Therefore, the presence of type III kerogen could at least partly be associated with terrestrial inputs associated with the above two fluvial systems building out into the marine depositional environment. The S_1-TOC cross-plot (Hunt 1996) revealed autochthonous hydrocarbon production with gas-generating potential (indigenous hydrocarbons with most of the S_1 values being low and ranging from 0.01 mg HC/g TOC to 0.1 mg HC/g TOC; Fig. 6d).

Thermal maturity

Thermal maturity of sedimentary organic matter is another crucial parameter for the characterization of source rocks, since their hydrocarbon generation potential changes with thermal maturation and the related loss of functional groups (Peters et al. 2005; Zieger et al. 2018). In the present study, the thermal maturity is determined by Rock–Eval PI and T_{max} measurements. An initial assessment of the degree of thermal maturity reached by the studied sediments is provided by T_{max} values. To be reliable, we used T_{max} values in our plots merely for the samples with S_2 values greater than 0.2 mg HC/g rock. Thus, T_{max} values from the samples with negligible organic richness and very low values for source rock potential were not taken into consideration, because such values cannot be considered as accurate (Peters and Cassa 1994). All reliable samples reach a relatively narrow range of T_{max} values from 400 to 417 °C (Table 1, Fig. 7a,b) indicating low thermal maturity and the presence of a large portion of unconverted original organic matter. Based on the HI-T_{max} plot (Espitalié et al. 1985), this pattern is further reflected in the kerogen type determination with a dominant gas-prone, type III kerogen distribution within the immature oil-window stage (Fig. 7a). Moreover, the PI-T_{max} cross-plot, which is also used to assess thermal maturity, clearly indicates that the examined upper Messinian sedimentary sequence is immature with respect to oil generation (Fig. 7b). Thus, it can be assumed that the results represent the initial quality of the organic matter. The determination of thermal maturity could be supported by additional geochemical analyses, such as vitrinite reflectance (Ro%) and/or Thermal Alteration Index (TAI) (Peters 1986). However, the studied profile corresponds to a continuous short sedimentary sequence, and therefore significant trends related to changes in regional thermal maturation level cannot be expected. Overall, these deposits have not experienced high temperature during burial and most likely contain very little charcoal or recycled material from older mature rocks. However, thermal maturity and hydrocarbon contribution to working petroleum systems might be enabled for Late Miocene intervals in deeper parts of the basin, where greater burial depths are reached.

Sedimentary basin dynamics: implications for the onshore depositional environment and petroleum play assessment

The studied samples of Plouti section belong to a mixed siliciclastic-carbonate sequence, which contain gas-prone (Type III kerogen) organic material, but they have not attained adequate thermal burial maturity. These samples are mainly representative of thin, clay organic-rich layers interbedded with massive sandstone and limestone packages. However, even in some of the sandy limestones, terrestrial organic particles could be identified, leading to elevated concentrations of TOC in these intervals. Generally, productivity (Totman Parrish and Curtis 1982; Pedersen and Calvert 1990), preservation (Demaison and Moore 1980; Demaison 1991; Vasiliev et al. 2019), sedimentation rate (Ibach 1982; Creaney and Passey 1993), and salinity influence (Horsfield et al. 1994; Yang and Schulz 2019) are typically considered as the most important factors controlling the organic matter and TOC enrichment in petroleum source rocks (Littke et al. 1997). In Plouti section, organic matter is more abundant in the more siliciclastic parts of the section and less common in the more calcareous intervals. This is evident at the outcrop scale, where the organic matter- and silty clay-rich intervals are interbedded with organic matter-lean and more calcareous intervals. This observation indicates that nutrient supply and thus bio-productivity (Nixon et al. 1986; Van der Zwaan and Jorissen 1991) during that interval were correlated with the deposition of siliciclastic material leading to higher accumulation of organic matter in the sediment. In case of slightly oxygenated bottom waters were still present, increased clastic (i.e., clays) sedimentation would increase both

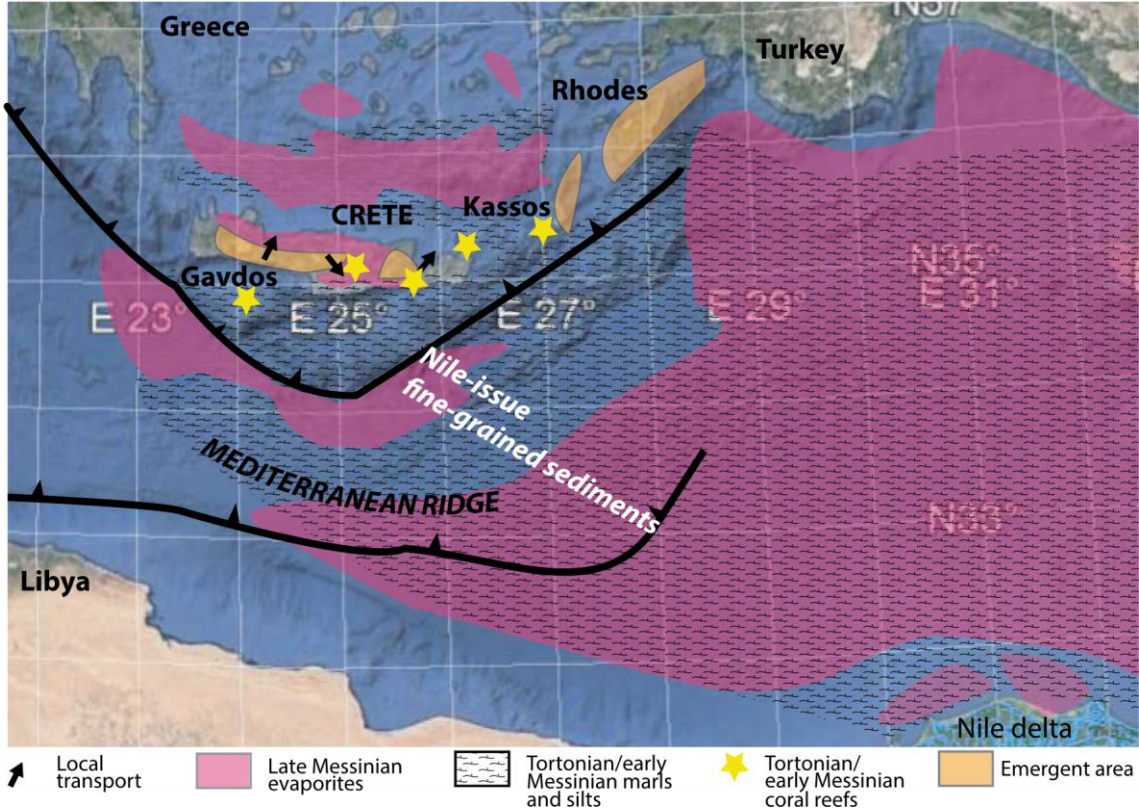

the burial efficiency and the potential of organic matter preservation by insulating the organic matter and shifting the oxic-anoxic boundary within the sediment closer to the sediment–water interface. The above interpretation leads to the

Fig. 8 Simplified paleogeographic map of the Hellenic subduction zone during the late Miocene. Coral reef and sediment distribution data obtained from Tsaparas and Marcopoulou-Diacantoni (2005), Brachert et al. (2006), Popov et al. (2006), Antonarakou et al. (2007), Brachert et al. (2007), and Perrin and Bosellini (2013)

lagoonal environmental concept, where a distinct influence of regional freshwater can be expected (e.g., Drinia et al. 2004, 2007) (Fig. 8). Particularly, the terrestrial inputs (e.g., plumes of fine sediments and nutrients) might originate from the northern African margin, which was the closest landmass during the Miocene (Robertson et al. 2012) and high amounts of clastic material were shed into the eastern Mediterranean basin through the Nile Delta (Sestini 1989; Hawie et al. 2013). This scenario is in accordance with the recent findings of Grohmann et al. (2018, 2019), where similar late Miocene clastic sediments derived from the Nile Delta and/ or the Levant margin, have been also characterized as gaseous source rocks onshore and offshore Cyprus.

Respecting the paleogeographic setting of Crete during the middle-late Miocene, characterized by local and regional factors (e.g., horst and graben stuctures, barrier effect and existence of restricted basins before the MSC, strong terrestrial influence with long distance transport of fine sediments and nutrients from the Nile, marine diagenesis; Fassoulas 2001; Antonarakou et al. 2007, 2019; Zachariasse et al. 2011; Zelilidis et al. 2016; Moissette et al. 2018; Kontakiotis et al. 2019), it can be assumed that similar constellations allowed the deposition of source rocks in several fore-arc basins between Crete and Mediterranean Ridge. However, strong lateral variations in the thickness of the salt layer in the upper deforming sequence (Late Miocene evaporites) between the western and the eastern foreland basins (Maravelis et al. 2015b), along with the local presence of mud diapirism (volcanoes), the diverse trap styles (stratigraphic and structural traps; Pantopoulos et al. 2013; Pantopoulos and Zelilidis, 2014), and the unusually great thickness and diverse character (various lithotypes) of the sedimentary infill differentiate the Mediterranean Ridge from most other accretionary complexes. All these very critical attributes can result to the recognition of several potential hydrocarbon plays in the eastern Mediterranean Sea. Particularly for the study area, where the four ingredients of a good petroleum system namely source, reservoir, trap and seal (Fig. 9) appear to occur (Maravelis et al. 2015b, 2016), it is recommended that the Greek authorities (Ministry of Environment, Energy and Climate Change) proceed with additional extensive onshore geological studies and detailed offshore seismic surveys to explore the existence of hydrocarbons around Crete Island, where the sedimentary succession has been more deeply buried, experienced a higher thermal evolution, and therefore might have matured sufficiently to enter the oil

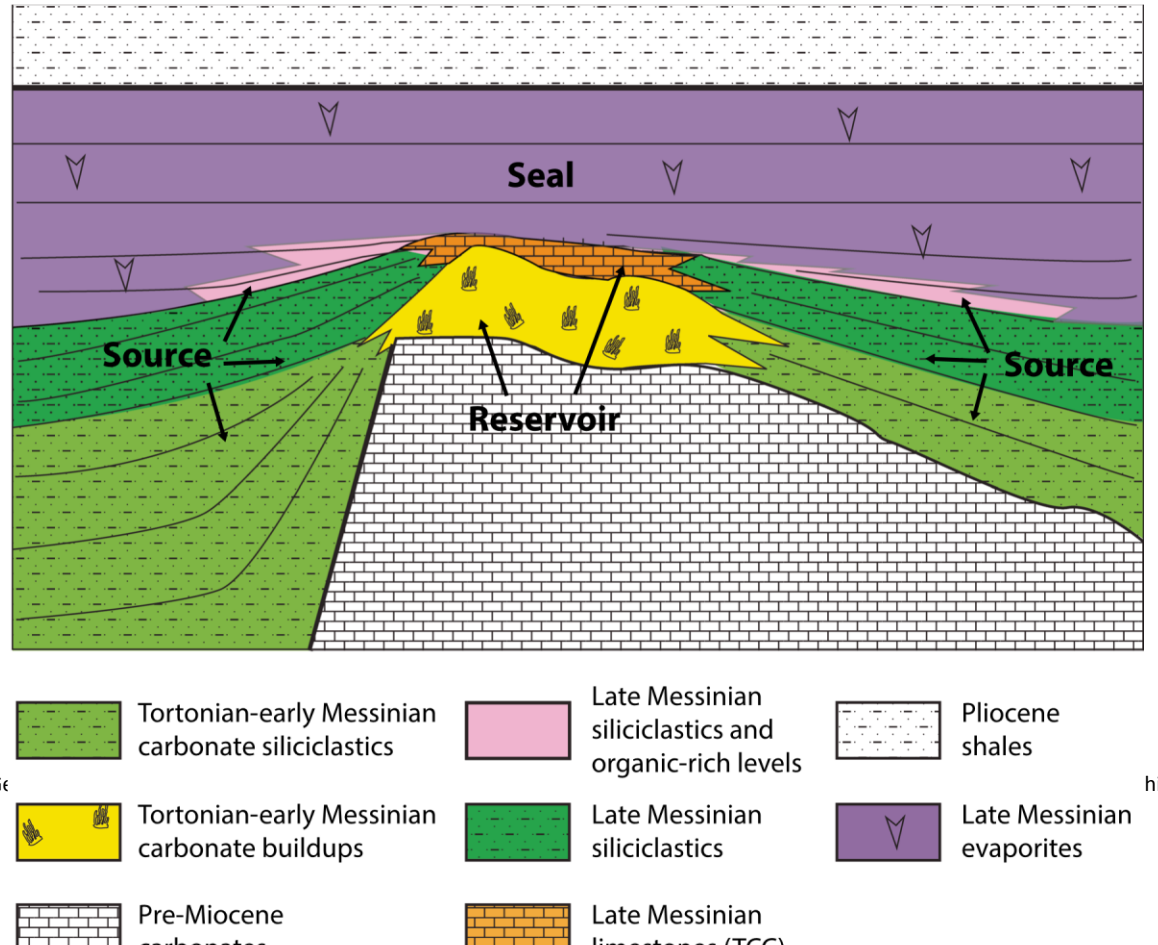

Fig. 9 Ge his study,

highlighting the relationship between the stratigraphic development of sedimentary sequences and the southwestern margin of the eastern Mediterranean petroleum system. The Plouti section, which corresponds to the lower part of the gypsum-TCC association, is not to scale and, only provides a conceptual organisation of Late Miocene source to trap sediments

generation zone. On this regard, remote sensing, seismic and wire-line log data, as well as cores and fluid samples from wells should be integrated to define the exact thickness and lateral extent of the possible seal, reservoir and source rocks, and the trap style.

Conclusions

The siliciclastic sub-salt sedimentary succession of the Plouti section exposed in the Heraklion basin (central Crete, eastern Mediterranean) was analyzed in order to evaluate the origin, type and maturation level of organic matter, as well as to assess the depositional environment. The geochemical results establish a potential regional Messinian gaseous source rock and analysis details its characteristics in terms of the total content of organic matter, its type, quality, and maturity level, along with the analysis of their generative potential. The TOC content of several samples is more than 0.5 wt % indicating some hydrocarbon generating potential, with both poor to fair (0.5% < TOC < 1.0%) and good (TOC > 1.0%) potential. Rock–Eval parameters reveal the occurrence of source rocks with poor to fair and/or good (organic-rich sediments) hydrocarbon generating potential, characterized by gas-prone kerogen, Type III. Although the investigated sedimentary rocks have sufficient TOC contents and HP values, and contain gas-prone organic material, they have not attained adequate thermal maturity at the study location, as the sedimentary overburden was not sufficient to reach the beginning of the oil window. The immature pre-evaporitic interval identified here could be considered as a potential source of biogenic gas, which is produced at shallow burial depths.

Acknowledgements This research has been co-financed by the European Union (European Social Fund–ESF) and Greek national funds through the Operational Program "Education and Lifelong Learning" of the National Strategic Reference Framework (NSRF) -Research Funding Program: THALIS–UOA-"Messinian Salinity Crisis: the greatest Mediterranean environmental perturbation and its repercussions to the biota" (MEDSALC) MIS: 375405. Constructive comments by two anonymous reviewers have been essential in improving this manuscript, and Prof. Dr. Attila Çiner (Editor in Chief) is thanked for his editorial handling.

References

Antonarakou A, Drinia H, Tsaparas N, Dermitzakis MD (2007) Micropaleontological parameters as proxies of late Miocene surface water properties and paleoclimate in Gavdos Island, eastern Mediterranean. Geodiversitas 29:379–399

Antonarakou A, Kontakiotis G, Vasilatos C, Besiou E, Zarkogiannis S,
Drinia H, Mortyn PG, Tsaparas N, Makri P, Karakitsios V (2019) Evaluating the effect of marine diagenesis on Late Miocene preevaporitic sedimentary successions of eastern Mediterranean Sea. IOP Conf Ser Earth Environ Sci 221:012051. https ://doi. org/10.1088/1755-1315/221/1/01205 1

Behar F, Beaumont V, Penteado HL, De B (2001) Technologie RockEval 6: performances et développements. Oil Gas Sci Technol Rev IFP 56:111–134

Ben-Avraham Z, Schattner U, Lazar M, Hall J, Ben-Gai Y, Neev D, Reshef M (2006) Segmentation of the Levant continental margin, eastern Mediterranean. Tectonics 25:TC5002

Bertello F, Harby H, Brandolese S (2016) Egypt: Zohr, an outstanding gas discovery in a new deep-water hydrocarbon play. Paper presented at the 8th Mediterranean offshore conference and exhibition, Alexandria, Egypt, pp 1–10

Bertoni C, Kirkham C, Cartwright J, Hodgson N, Rodriguez K (2017) Seismic indicators of focused fluid flow and cross-evaporitic seepage in the Eastern Mediterranean. Mar Petrol Geol 88:472–488

Bohrmann G, Aljuhne A, Dehning K, Ferreira C, Feseker T, Gürcan ES, Hacioglu E, Leymann T, Meinecke G, Pape T, Renken J, Römer M, Spiesecke U, von Wahl T (2014) Report and preliminary results of R/V POSEIDON cruise P462, Izmir—Izmir, 28 October–21 November, 2013. Gas hydrate dynamics of mud volcanoes in the submarine anaximander mountains (Eastern Mediterranean), vol 300. http://publi catio ns.marum .de/2346/

Bou Daher S, Ducros M, Michel P, Hawie N, Nader FH, Littke R (2016) 3D thermal history and maturity modelling of the Levant Basin and its eastern margin, offshore–onshore Lebanon. Arab J Geosci. https ://doi.org/10.1007/s1251 7-016-2517-4

Bourillot R, Vennin E, Rouchy JM, Durlet C, Rommevaux V, Kolodka C, Knap F (2010) Structure and evolution of a Messinian mixed carbonate siliciclastic platform: the role of evaporites (Sorbas Basin, South-east Spain). Sedimentology 57:477–512

Bourli N, Kokkaliari M, Iliopoulos I, Pe-Piper G, Piper DJW, Maravelis AG, Zelilidis A (2019a) Mineralogy of siliceous concretions, cretaceous of ionian zone, western Greece: Implication for diagenesis and porosity. Mar Petrol Geol 105:45–63. https :// doi.org/10.1016/j.marpe tgeo.2019.04.011

Bourli N, Pantopoulos G, Maravelis AG, Zoumpoulis E, Iliopoulos G, Pomoni-Papaioannou F, Kostopoulou S, Zelilidis A (2019b) Late Cretaceous to early Eocene geological history of the eastern Ionian Basin, southwestern Greece: a sedimentological approach. Cretac Res 98:47–71. https ://doi.org/10.1016/j.cretr es.2019.01.026

Brachert TC, Reuter M, Felis T, Kroeger KF, Lohmann G, Micheels A, Fassoulas C (2006) *Porites* corals from Crete (Greece) open a window into Late Miocene (10 Ma) seasonal and interannual climate variability. Earth Planet Sci Lett 245:81–94

Brachert TC, Vescogni A, Bosellini FR, Reuter M, Mertz-Kraus R (2007) High salinity variability during the early Messinian revealed by stable isotope signatures from vermetid and *Halimeda* reefs of the Mediterranean region. Geol Romana 40:1–16

Bruneton A, Konofagos E, Foscolos A (2011) Economic and geopolitical importance of Eastern Mediterranean gas fields for Greece and the E. U. Emphasis on the probable natural gas deposits occurring in the Libyan Sea within the Exclusive Economic Zone of Greece. Mineral Wealth 160:7–30

Burwood R, De Witte S, Mycke B, Paulet J (1995) Petroleum geochemical characterization of the Lower Congo coastal basin Bucomazi Formation. In: Katz BJ (ed) Petroleum Source Rocks. Springer, Berlin, pp 235–263

Camerlenghi A, Cita MB (1987) Setting and tectonic evolution of some Eastern Mediterranean deep-sea basins. Mar Geol 75:31–55

Camerlenghi A, Cita MB, Hieke W, Ricchiuto T (1992) Geological evidence for mud diapirism on the Mediterranean Ridge accretionary complex. Earth Planet Sci Lett 109:493–504

Chaumillon E, Mascle J, Hoffmann HJ (1996) Deformation of the western Mediterranean Ridge: importance of Messinian evaporitic formations. Tectonophysics 263:163–190

CIESM (2008) The Messinian Salinity Crisis from mega-deposits to microbiology—a consensus report. In: Briand F (ed) CIESM workshop monographs, vol 33. CIESM Publisher, Monaco, pp 1–168

Cita MB, Ryan WBF, Paggi L (1981) Prometheus mud breccia: an example of shale diapirism in the Western Mediterranean Ridge. Ann Géol Pays Hellén 30:543–569

Cornée JJ, Saint Martin JP, Conesa G, Münch P, André JP, Saint Martin S, Roger S (2004) Correlations and sequence stratigraphic model for Messinian carbonate platforms of the western and central Mediterranean. Int J Earth Sci 93:621–633

Creaney S, Passey QR (1993) Recurring patterns of total organic carbon and source rock quality within a sequence stratigraphic framework. AAPG Bull 77:386–401

Cronin BT, Ivanov MK, Limonov AF, Egorov A, Akhmanov GG, Akhmetjanov AM, Kozlova E, Shipboard Scientific Party TTR-5 (1997) New discoveries of mud volcanoes on the Eastern Mediterranean Ridge. J Geol Soc Lond 154:173–182

Demaison G (1991) Anoxia vs. productivity: what controls the formation of organic-carbon-rich sediments and sedimentary rocks? AAPG Bull 74:454–466

Demaison G, Moore GT (1980) Anoxic environments and oil source bed genesis. Org Geochem 2:9–31

Dembicki H Jr (2009) Three common source rock evaluation errors made by geologists during prospect or play appraisals. Am Assoc Pet Geol Bull 93:341–356

Dolan P, Burggraf D, Soofi K, Fitzsimmons R, Aydemir E, Senneseth O, Strickland L (2004) Challenges to exploration in frontier basins—the Barbados accretionary prism. Paper presented at the AAPG international conference, October 24–27, Cancun, Mexico, pp 1–6

Drinia H, Antonarakou A, Tsaparas N, Dermitzakis MD, Kontakiotis G (2004) Foraminiferal record of environmental changes: preevaporitic diatomaceous sediments from Gavdos Island, southern Greece. Bull Geol Soc Greece 36:782–791

Drinia H, Antonarakou A, Tsaparas N, Kontakiotis G (2007) Palaeoenvironmental conditions preceding the Messinian Salinity Crisis: a case study from Gavdos Island. Geobios 40:251–265

Drinia H, Antonarakou A, Kontakiotis G (2008) On the occurrence of Early Pliocene marine deposits in the Ierapetra Basin, Eastern Crete, Greece. Bull Geosci 83:63–78

Dymann TS, Palacas JG, Tysdal RG, Perry WJ, Pawlewicz MJ (1996) Source rock potential of Middle Cretaceous rocks in southwestern Montana. AAPG Bull 80:1177–1184

Elia C, Konstantopoulos P, Maravelis AG, Zelilidis A (2013) The tectono-stratigraphic evolution of SE Mediterranean with emphasis on Herodotus Basin prospectivity for the development of hydrocarbon fields. Bull Geol Soc Greece 47:1970–1979

Escalona A, Mann P, Bingham L (2008) Hydrocarbon exploration plays in the Great Caribbean region and neighboring provinces. Paper presented at the AAPG annual convention, San Antonio Texas, April 20–23. Search and Discovery Article # 10047

Esestime P, Hewitt A, Hodgson N (2016) Zohr—a newborn carbonate play in the Levantine Basin, East-Mediterranean. First Break 34:87–93

Espitalié J, Laporte JL, Madec M, Marquis F, Leplat P, Paulet J, Boutefeu A (1977) Méthode rapide de caractérisation des roches mères, de leur potentiel pétrolier et de leur degré d'évolution. Rev Inst Fr Pét 32:23–42

Espitalié J, Deroo G, Marquis F (1985) La pyrolyse Rock-Eval et ses applications. Première partie. Rev Inst Fr Pét 40:73–89

Esteban M (1979) Significance of the upper Miocene reefs in the Western Mediterranean. Palaeogeogr Palaeoclimatol Palaeoecol 29:169–188

Fassoulas C (2001) The tectonic development of a Neogene basin at the leading edge of the active European margin: the Heraklion basin, Crete, Greece. J Geodyn 31:49–70

Foscolos A, Konophagos E, Bruneton A (2012) The occurrence of converging plates, mud flow volcanoes and accretionary prism complexes in the Mediterranean Ridge. Their relationship to possible hydrocarbon accumulations off shore Crete. A new perspective for oil and natural gas resources of Greece. Mineral Wealth 165:7–26

Frey-Martinez JCJ, Hall B, Huuse M (2007) Clastic intrusion at the base of deep-water sands: a trap-forming mechanism in the Eastern Mediterranean. In: Hurst A, Cartwright J (eds) Sand injectites: implications for hydrocarbon exploration and production, vol 87. AAPG Memoir, Tulsa, pp 49–63

Gao H, Tong X, Wen Z, Wang Z (2019) The tectonic evolution of the eastern Mediterranean basin and its control on hydrocarbon distribution. J Petrol Sci Eng 178:389–407

Garcia-Castellanos D, Estrada F, Jiménez-Munt I, Gorini C, Fernàndez M, Vergés J, De Vicente R (2009) Catastrophic flood of the Mediterranean after the Messinian salinity crisis. Nature 462:778–781

Gardosh MA, Druckman Y (2006) Seismic stratigraphy, structure and tectonic evolution of the Levantine Basin, offshore Israel. Geol Soc Lond Spec Publ 260:201–227

Gardosh MA, Garfunkel Z, Druckman Y, Buchbinder B (2010) Tethyan rifting in the Levant region and its role in early Mesozoic crustal evolution. J Geol Soc Lond 341:9–36

Ghalayini R, Daniel JM, Homberg C, Nader FH, Comstock JE (2014) Impact of Cenozoic strike-slip tectonics on the evolution of the northern Levant Basin (offshore Lebanon). Tectonics 33:2121–2142

Gladstone R, Flecker R, Valdes P, Lunt D, Markwick P (2007) The Mediterranean hydrologic budget from a Late Miocene global climate simulation. Palaeogeogr Palaeoclimatol Palaeoecol 251:254–267

Grohmann S, Fietz SW, Littke R, Daher SB, Romero-Sarmiento M-F, Nader FH, Baudin F (2018) Source rock characterization of mesozoic to cenozoic organic matter rich marls and shales of the Eratosthenes Seamount, Eastern Mediterranean Sea. Oil Gas Sci Technol Rev IFP Energ Nouv 73:49. https: //doi.org/10.2516/ ogst/20180 36

Grohmann S, Romero-Sarmiento M-F, Nader FH, Baudin F, Littke R (2019) Geochemical and petrographic investigation of Triassic and Late Miocene organic-rich intervals from onshore Cyprus, Eastern Mediterranean. Int J Coal Geol 209:94–116. https: //doi. org/10.1016/j.coal.2019.05.001

Grothe A, Andreetto F, Reichart G-J, Wolthers M, Van Baak CGC, Vasiliev I, Stoica M, Sangiorgi F, Middelburg JJ, Davies GR, Krijgsman W (2020) Paratethys pacing of the Messinian Salinity Crisis: low salinity waters contributing to gypsum precipitation? Earth Planet Sci Lett 532:116029. https: //doi.org/10.1016/j. epsl.2019.11602 9

Haese RR, Hensen C, de Lange GJ (2006) Pore water geochemistry of Eastern Mediterranean mud volcanoes: Implications for fluid transport and fluid origin. Mar Geol 225:191–208

Hawie N, Gorini C, Deschamps R, Nader FH, Montadert L, Granjeon D, Baudin F (2013) Tectono-stratigraphic evolution of the northern Levant Basin (offshore Lebanon). Mar Petrol Geol 48:392–410

Hilgen F, Krijgsman W (1999) Cyclostratigraphy and astrochronology of the Tripoli diatomite Formation (pre-evaporite Messinian, Sicily, Italy). Terra Nova 11:16–22

Hilgen FJ, Kuiper K, Krijgsman W, Snel E, van der Laan E (2007) Astronomical tuning as the basis for high resolution chronostratigraphy: the intricate history of the Messinian Salinity Crisis. Stratigraphy 4:231–238

Horsfield B, Curry DJ, Bohacs K, Littke R, Rullkötter J, Schenk HJ, Radke M, Schaefer RG, Carroll AR, Isaksen G, Witte EG (1994) Organic geochemistry of freshwater and alkaline lacustrine sediments in the Green River Formation of the Washakie Basin, Wyoming, USA. Org Geochem 22:415–440

Hsü KJ, Ryan WBF, Cita MB (1973) Late Miocene desiccation of the Mediterranean. Nature 242:240–244

Huguen C, Mascle J, Chaumillon E, Woodside JM, Benkhelil J, Kopf A, Volokonskaia A (2001) Deformation styles of the eastern Mediterranean Ridge and surroundings from combined swatch mapping and seismic reflection profiling. Tectonophysics 343:21–47

Huguen C, Mascle J, Chaumillon E, Kopf A, Woodside J, Zitter T (2004) Structural setting and tectonic control of mud volcanoes from the Central Mediterranean Ridge (Eastern Mediterranean). Mar Geol 209:245–263

Huguen C, Chamot-Rooke N, Loubrieu B, Mascle J (2006) Morphology of a precollisional, salt-bearing, accretionary complex: the Mediterranean Ridge (East Mediterranean). Mar Geophys Res 27:61–75

Hunt JM (1967) The origin of petroleum in carbonate rocks. In: Chilingar GV, Bissel HJ, Fairbridge RW (eds) Developments in sedimentology, 9B. Carbonate rocks: physical and chemical aspects. Elsevier, New York, pp 225–251

Hunt JM (1979) Petroleum geochemistry and geology, 1st edn. W.H. Freeman and Company, San Francisco

Hunt JM (1996) Petroleum geochemistry and geology, 2nd edn. W.H. Freeman and Company, New York

Hüsing SK, Kuiper KF, Link W, Hilgen FJ, Krijgsman W (2009) The upper Tortonian-lower Messinian at Monte dei Corvi (Northern Apennines, Italy): completing a Mediterranean reference section for the Tortonian Stage. Earth Planet Sci Lett 282:140–157

Ibach LEJ (1982) Relationship between sedimentation rate and total organic carbon content in ancient marine sediments. AAPG Bull 66:170–188

Jackson KS, Hawkins PJ, Bennett AJR (1985) Regional facies and geochemical evaluation of southern Denison Trough, Queensland. APPEA J 20:143–158

Jones RW (1984) Comparison of carbonate and shale source rocks. In: Palacas JG (ed) Petroleum geochemistry and source rock potential of carbonate rocks, vol 18. AAPG Stud. Geol., Tulsa, pp 163–180

Jones W, Tripathi A, Rajagopal LR, Williams A (2011) Accretionary prisms-plate tectonics-hydrocarbons. Petroleum prospectivity of the West Timor trough. https ://www.pnron line.com.au/artic le.php/127/150

Karakitsios V (2013) Western Greece and Ionian petroleum systems. AAPG Bull 97:1567–1595

Karakitsios V, Rigakis N (1996) New oil source rocks cut in Greek Ionian basin. Oil Gas J 94:56–59

Karakitsios V, Rigakis N (2007) Evolution and petroleum potential of Western Greece. J Petrol Geol 30:197–218

Karakitsios V, Rigakis N, Bakopoulos I (2001) Migration and trapping of the Ionian series hydrocarbons (Epirus, NW Greece). Bull Geol Soc Greece 34:1237–1245

Karakitsios V, Roveri M, Lugli S, Manzi V, Gennari R, Antonarakou A, Triantaphyllou M, Agiadi K, Kontakiotis G (2013) Remarks on the Messinian evaporates of Zakynthos Island (Ionian Sea, Eastern Mediterranean). Bull Geol Soc Greece 47(1):146–156

Karakitsios V, Cornée JJ, Tsourou T, Moissette P, Kontakiotis G, Agiadi K, Manoutsoglou E, Triantaphyllou M, Koskeridou E, Drinia H, Roussos D (2017a) Messinian salinity crisis record under strong freshwater input in marginal, intermediate, and deep environments: the case of the North Aegean. Palaeogeogr Palaeoclimatol Palaeoecol 485:316–335

Karakitsios V, Roveri M, Lugli S, Manzi V, Gennari G, Antonarakou A, Triantaphyllou M, Agiadi K, Kontakiotis G, Kafousia N, de Rafelis M (2017b) A record of the Messinian salinity crisis in the eastern Ionian tectonically active domain (Greece, eastern Mediterranean). Basin Res 29:203–233

Kissel C, Laj C (1988) The Tertiary geodynamic evolution of the Aegean arc: a paleomagnetic reconstruction. Tectonophysics 146:183–201

Klein GD, Zuniga-Rivero J, Hay-Roe H, Alvarez-Calderon E (2011) Mesozoic/Cenozoic tectonic evolution, basin fairways and play opportunities of Peru. Houst Geol Soc Bull 54:45–47

Kontakiotis G, Karakitsios V, Mortyn PG, Antonarakou A, Drinia H, Anastasakis G, Agiadi K, Kafousia N, De Rafelis M (2016) New insights into the early Pliocene hydrographic dynamics and their relationship to the climatic evolution of the Mediterranean Sea. Palaeogeogr Palaeoclimatol Palaeoecol 459:348–364

Kontakiotis G, Besiou E, Antonarakou A, Zarkogiannis S, Kostis A, Mortyn PG, Moissette P, Cornée JJ, Schulbert C, Drinia H, Anastasakis G, Karakitsios V (2019) Decoding sea surface and paleoclimate conditions in the eastern Mediterranean over the Tortonian-Messinian Transition. Palaeogeogr Palaeoclimatol Palaeoecol 534:109312

Kontopoulos N, Zelilidis A, Frydas D (1996) Late Neogene sedimentary and tectonostratigraphic evolution of northwestern Crete island, Greece. Neues Jahrb Geol Paläontol Abh 202:287–311

Kopf A, Mascle J, Klaeschen D (2003) The Mediterranean Ridge: A mass balance across the fastest growing accretionary complex on Earth. J Geophys Res 108(B8):2372

Kreemer C, Chamot-Rooke N (2004) Contemporary kinematics of the Southern Aegean and the Mediterranean Ridge. Geophys J Int 157:1377–1392

Krijgsman W, Hilgen FJ, Marabini S, Vai GB (1999) New paleomagnetic and cyclostratigraphic age constraints on the Messinian of the Northern Apennines (Vera del Gesso Basin, Italy). Mem Soc Geol Ital 54:25–33

Krijgsman W, Stoica M, Vasiliev I, Popov VV (2010) Rise and fall of the Paratethys Sea during the Messinian Salinity Crisis. Earth Planet Sci Lett 290(1–2):183–191. https ://doi.org/10.1016/j. epsl.2009.12.020

Krois P, Hannke K, Novotny B, Bayoumi T, Hussein H, Tari G (2010) The emerging deepwater province of Northwest Egypt. Paper presented at the AAPG international conference and exhibition, Rio de Janeiro, Brazil, Search and Discovery Article #10241

Lafargue E, Marquis F, Pillot D (1998) Rock-eval 6 applications in hydrocarbon exploration, production, and soil contamination studies. Oil Gas Sci Technol Rev IFP Energ Nouv 53:421–437

Langereis CG, Hilgen FJ (1991) The Rossello composite: a Mediterranean and global reference section for the Early to early Late Pliocene. Earth Planet Sci Lett 104:211–225

Le Pichon X, Chamot-Rooke N, Lallemant S, Noomen R, Veis G (1995) Geodetic determination of the kinematics of central Greece with respect to Europe: implications for eastern Mediterranean tectonics. J Geophys Res 100:12675–12690

Leila M, Moscariello A, Kora M, Mohamed A, Samankassou E (2020) Sedimentology and reservoir quality of a Messinian mixed siliciclastic-carbonate succession, onshore Nile Delta, Egypt. Mar Pet Geol 112:104076

Limonov AF, Woodside JM, Cita MB, Ivanov MK (1996) The Mediterranean Ridge and related mud diapirism: a background. Mar Geol 132:7–19

Littke R, Baker D, Rullkötter J (1997) Deposition of petroleum source rocks. In: Welte DH, Horsfield B, Baker DR (eds) Petroleum and basin evolution. Springer, Berlin, pp 271–333

Loncke L, Mascle J, Parties Fanil Scientific (2004) Mud volcanoes, gas chimneys, pockmarks and mounds in the Nile deep-sea fan (Eastern Mediterranean): geophysical evidence. Mar Petrol Geol 21:669–689

Lykousis V, Alexandri S, Woodside J, de Lange G, Dählmann A, Perissoratis C, Heeschen K, Ioakim C, Sakellariou D, Nomikou P, Rousakis G, Casas D, Ballas D, Ercilla G (2009) Mud volcanoes and gas hydrates in the Anaximander mountains (Eastern Mediterranean Sea). Mar Petrol Geol 26:854–872

Macgregor DS (2012) The development of the Nile drainage system: integration of onshore and offshore evidence. Pet Geosci 18:417–431

Mann P, Galagan L, Gordon MP (2003) Tectonic settings of the world's giant oil and gas fields. In: Halbouty MT (ed) Giant oil and gas fields of the decade 1990–1999, vol 78. AAPG Memoir, Tulsa, pp 15–105

Mantovani E, Viti M, Albarello D, Tamburelli C, Babbucci D, Cenni N (2000) Role of kinematically induced horizontal forces in Mediterranean tectonics: insights from numerical modeling. J Geodyn 30:287–320

Manzi V, Lugli S, Roveri M, Schreiber BC, Gennari G (2011) The Messinian "Calcare di Base" (Sicily, Italy) revisited. Geol Soc Am Bull 123:347–370

Manzi V, Gennari R, Lugli S, Roveri M, Scaletta N, Schreiber B (2012) High frequency cyclicity in the Mediterranean Messinian evaporites: evidence for solar-lunar climate forcing. J Sed Res 82:991–1005

Manzi V, Gennari R, Hilgen F, Krijgsman W, Lugli S, Roveri M, Sierro FJ (2013) Age refinement of the Messinian salinity crisis onset in the Mediterranean. Terra Nova 25:315–322

Maravelis AG, Zelilidis A (2011) Geometry and sequence stratigraphy of the Late Eocene-Early Oligocene shelf and basin floor to slope turbidite systems, Lemnos Island, NE Greece. Stratigr Geol Correl 19:205–220

Maravelis AG, Makrodimitras G, Zelilidis A (2012) Hydrocarbon prospectivity in western Greece. Oil Gas-Eur Mag 38:84–89

Maravelis AG, Makrodimitras G, Pasadakis N, Zelilidis A (2014) Stratigraphic evolution and source rock potential of a Lower Oligocene to Lower-Middle Miocene continental slope system, Hellenic Fold and Thrust Belt, Ionian Sea, northwest Greece. Geol Mag 151:394–413

Maravelis AG, Koukounya A, Tserolas P, Pasadakis N, Zelilidis A (2015a) Geochemistry of Upper Miocene-Lower Pliocene source rocks in the Hellenic Fold and Thrust Belt, Zakynthos Island, Ionian Sea, western Greece. Mar Petrol Geol 66:217–230

Maravelis A, Manutsoglu E, Konstantopoulos P, Pantopoulos G, Makrodimitras G, Zoumpouli E, Zelilidis A (2015b) Hydrocarbon plays and prospectivity of the Mediterranean Ridge. Energy Sour Part A Recovery Util Environ Eff 37(4):347–355

Maravelis AG, Panagopoulos G, Piliotis J, Pasadakis N, Manoutsoglou E, Zelilidis A (2016) Pre-messinian (sub-salt) source-rock potential on back-stop basins of the hellenic trench system (Messara Basin, Central Crete, Greece). Oil Gas Sci Technol Rev IFP Energ Nouv 71:1–19

Maravelis AG, Boutelier D, Catuneanu O, Seymour KS, Zelilidis A (2017) A review of tectonics and sedimentation in a forearc setting: Hellenic Thrace Basin, North Aegean Sea and Northern Greece. Tectonophysics 674:1–19

Martín JM, Braga JC (1994) Messinian events in the Sorbas Basin in southeastern Spain and their implications in the recent history of the Mediterranean. Sed Geol 90:257–268

Meulenkamp JE (1979) Field guide to the Neogene of Crete. Dep Geol Pal Univ Athens Ser A32:1–31

Meulenkamp JE, van der Zwaan GJ, van Wamel WA (1994) On late Miocene to recent vertical motions in the Cretan segment of the Hellenic arc. Tectonophysics 234:53–72

Moforis L, Kostopoulou S, Panagopoulos G, Pyliotis I, Triantaphylou M, Manoutsoglou E, Zelilidis A (2013) Sedimentation processes and palaeographic evolution of Makrilia Pliocene deposits. SE Crete Bull Geol Soc Greece 47(1):216–225

Moissette P, Cornée JJ, Mannaï-Tayech B, Rabhi M, André JP, Koskeridou E, Méon H (2010) The western edge of the Mediterranean Pelagian Platform: a Messinian mixed siliciclastic-carbonate ramp in northern Tunisia. Palaeogeogr Palaeoclimatol Palaeoecol 285:85–103

Moissette P, Cornée JJ, Antonarakou A, Kontakiotis G, Drinia H, Koskeridou E, Tsourou T, Agiadi K, Karakitsios V (2018) Palaeoenvironmental changes at the Tortonian/Messinian boundary: a deep-sea sedimentary record of the eastern Mediterranean Sea. Palaeogeogr Palaeoclimatol Palaeoecol 505:217–233

Montadert L, Nikolaides S (2007) The geological structure of the Eratosthenes continental block and its margins with the Levantine and Herodotus Basins (Eastern Mediterranean) from new seismic reflection data. Paper presented at the AAPG European Region Conference, Athens, Greece

Montadert L, Nikolaides S, Semb PH, Lie Ø (2014) Petroleum systems offshore Cyprus. In: Marlow L, Kendall C, Yose L (eds) Petroleum systems of the tethyan region, vol 160. AAPG Special Volumes Memoir, Tulsa, pp 301–334

Natalicchio M, Dela Pierre F, Lugli S, Lowenstein TK, Feiner SJ, Ferrando S, Manz IV, Roveri M, Clari P (2014) Did late Miocene (Messinian) gypsum precipitate from evaporated marine brines? Insights from the Piedmont Basin (Italy). Geology 42:179–182

Needham D, Hosler J, Nowak S, Christensen C, Ffrench J (2013) The Tamar field from discovery to production. Paper presented at the AAPG European Regional Conference, Barcelona, Spain, AAPG Search and Discovery Article #90161

Nixon SW, Oviatt CA, Frithsen J, Sullivan B (1986) Nutrients and the productivity of estuarine and coastal marine ecosystems. J Limnol Soc S Afr 12:43–71

Olivet JL, Bonnin J, Beuzart P, Auzende JM (1982) Cinématique des plaques et paléogéographie: une revue. Bull Soc Geol Fr 24:875–892

Panagopoulos G, Pyliotis I, Zelilidis A, Spyridonos E, Hamdam H, Vafidis A, Manoutsoglou E (2011) 3D modeling of biogenic gasbearing Neogene deposits at Arkalochori region, Messara, Crete, Greece. Proceedings of IAMG, 5–9 September 2011, Saltzburg, pp 430–439

Pantopoulos G, Zelilidis A (2014) Eocene to Early Oligocene turbidite sedimentation in the SE Aegean (Karpathos Island, SE Greece): stratigraphy, facies analysis, nannofossil study, and possible hydrocarbon potential. Turk J Earth Sci 22:31–52

Pantopoulos G, Vakalas I, Maravelis AG, Zelilidis A (2013) Statistical analysis of turbidite bed thickness patterns from the Alpine fold and thrust belt of western and southeastern Greece. Sed Geol 294:37–57

Papanikolaou D, Vassilakis E (2010) Thrust faults and extensional detachment faults in Cretan tectono-stratigraphy: Implications for Middle Miocene extension. Tectonophysics 488:233–247

Pape T, Kasten S, Zabel M, Bahr A, Abegg F, Hohnerg HJ, Bohrmann G (2010) Gas hydrates in shallow deposits of the Amsterdam mud volcano, Anaximander Mountains, Northeastern Mediterranean Sea. Geo-Mar Lett 30:187–206

Pasadakis N, Dagounaki V, Chamilaki E, Vafidis A, Zelilidis A, Piliotis I, Panagopoulos G, Manoutsoglou E (2012) Organic geochemical evaluation of Neogene formations in Messara (Heraklion, Crete) basin as source rocks of biogenetic methane. Mineral Wealth 166:8–26

Pedersen T, Calvert S (1990) Anoxia vs. productivity: what controls the formation of organic-carbon-rich sediments and sedimentary rocks? AAPG Bull 74:454–466

Perrin C, Bosellini A (2013) The Late Miocene coldspot of z-coral diversity in the Mediterranean: patterns and causes. CR Palevol 12:245–255

Persad KM (2008) Petroleum geology and prospects of Trinidad and Tobago. Paper presented at the 100 years of petroleum in Trinidad and Tobago, pp 178–186. http://www.energy .gov.tt/content /
Cente nery_Pub_Krish na_Persa d.pdf

Peters KE (1986) Guidelines for evaluating petroleum source rock using programmed pyrolysis. Am Assoc Pet Geol Bull 70:318–329

Peters KE, Cassa MR (1994) Applied source rock geochemistry. In: Magoon LB, Dow WG (eds) The petroleum system-from source to Trap, vol 60. Am. Assoc. Petr. Geol. Mem., pp 93–120

Peters KE, Walters CC, Moldowan JM (2005) The biomarker guide. Biomarkers and isotopes in petroleum exploration and earth history, 2nd edn, vol 2. Cambridge University Press, Cambridge, p 683

Popov SV, Shcherba IG, Ilyina LB, Nevesskaya LA, Paramonova NP, Khondkarian SO, Magyar I (2006) Late Miocene to Pliocene palaeogeography of the Paratethys and its relation to the Mediterranean. Palaeogeogr Palaeoclimatol Palaeoecol 238:91–106

Praeg D, Unnithan V, Camerlenghi A (2007) PROJECT: HYDRAMED. Gas hydrate stability and prospectivity in the Mediterranean Sea. https ://www.dur.ac.uk/ey.go/gener al_publi c/AAPG_Newsl etter _June.pdf

Praeg D, Geletti R, Wardell N, Unnithan V, Mascle J, Migeon S, Camerlenghi A (2011) The Mediterranean Sea: a natural laboratory to study gas hydrate dynamics? Paper presented at the proceedings of the 7th international conference on gas hydrates (ICGH 2011), Edinburgh, Scotland, United Kingdom, July 17–21

Pyliotis I, Zelilidis A, Pasadakis N, Panagopoulos G, Manoutsoglou E (2013) Source rock potential of the late Miocene Metochia formation of Gavdos island, Greece. Bull Geol Soc Greece 43:871–879

Ratner M (2016) Natural gas discoveries in the Eastern Mediterranean. Congressional Research Service, Washington, DC, pp 1–15

Reillinger RE, McClusty SC, Oral MB, King RW, Toksoz MN (1997) Global positioning system measurements of present-day crustal movements in the Arabia-Africa-Eurasia plate collision zone. J
Geophys Res 102:9983–9999

Reuter M, Brachert TC, Kroeger KF (2006) Shallow-marine carbonates of the tropical–temperate transition zone: effects of hinterland climate and basin physiography (late Miocene, Crete, Greece). In: Pedley HM, Carannante G (eds) Cool-water carbonates: depositional systems and palaeoenvironmental controls, vol 255. Geol Soc. Spec. Publ., pp 157–178

Roberts G, Peace D (2007) Hydrocarbon plays and prospectivity of the Levantine Basin, offshore Lebanon and Syria from modern seismic data. GeoArabia 12:99–124

Robertson AHF (1998) Mesozoic-Tertiary tectonic evolution of the easternmost Mediterranean area: integration of marine and land evidence. Proc Ocean Drill Prog Sci Res 160:723–782

Robertson AHF, Kopf A (1998) Tectonic setting and processes of mud volcanism on the Mediterranean Ridge accretionary complex: evidence from Leg 160. Proc Ocean Drill Prog Sci Res 160:665–680

Robertson AHF, Parlak O, Ustaömer T (2012) Overview of the Palaeozoic-Neogene evolution of neotethys in the Eastern Mediterranean region (Southern Turkey, Cyprus, Syria). Petrol Geosci 18:381–404

Roveri M, Lugli S, Manzi V, Schreiber BC (2008) The Messinian Sicilian stratigraphy revisited: new insights for the Messinian salinity crisis. Terra Nova 20:483–488

Roveri M, Gennari G, Lugli S, Manzi V (2009) The terminal carbonate complex: the record of sea- level changes during the Messinian salinity crisis. GeoActa 8:63–77

Roveri M, Flecker R, Krijgsman W, Lofi J, Lugli S, Manzi V, Sierro FJ, Bertini A, Camerlenghi A, De Lange G, Govers R, Hilgen F, Hübscher C, Meijer PT, Stoica M (2014) The Messinian Salinity Crisis: past and future of a great challenge for marine sciences. Mar Geol 352:25–58

Sakellariou D, Tsampouraki-Kraounaki K (2019) Plio-Quaternary extension and strike-slip tectonics in the Aegean. In: Duarte JC (ed) Transform Plate Boundaries and Fracture Zones. pp 339–374. https ://doi.org/10.1016/B978-0-12-81206 4-4.00014 -1

Samuel OJ, Cornford C, Jones M, Adekeye OA, Akande SO (2009) Improved understanding of the petroleum systems of the Niger Delta Basin, Nigeria. Org Geochem 40:461–483

Schenk CJ, Kirschbaum MA, Charpentier RR, Klett TR, Brownfield ME, Pitman JK, Cook TA, Tennyson ME (2010) Assessment of undiscovered oil and gas resources of the Levant Basin Province, Eastern Mediterranean. US Geol Surv Fact Sheet 2010–3014:1–4

Segev A, Rybakov M (2010) Effects of Cretaceous plume and convergence, and Early Tertiary tectonomagmatic quiescence on the central and southern Levant continental margin. J Geol Soc Lond 167:731–749

Semb PH (2009) Possible seismic hydrocarbon indicators in offshore Cyprus and Lebanon. GeoArabia 14:49–66

Sestini G (1989) Nile Delta: a review of depositional environments and geological history. Geol Soc Spec Publ 41:99–127

Steinberg J, Gvirtzman Z, Folkman Y, Garfunkel Z (2011) Origin and nature of the rapid late Tertiary filling of the Levant Basin. Geology 39:355–358

Tamborrino L, Himmler T, Elvert M, Conti S, Gualtieri AF, Fontana D, Bohrmann G (2019) Formation of tubular carbonate conduits at Athina mud volcano, eastern Mediterranean Sea. Mar Petrol

Geol 107:20–31
ten Veen JH, Postma G (1999) Neogene tectonics and basin fill patterns in the Hellenic outer-arc (Crete, Greece). Basin Res 11:223–241
Tissot BP, Welte DH (1984) Petroleum formation and occurrence, 2nd edn. Springer, Berlin
Tissot B, Durand B, Espitalié J, Combaz A (1974) Influence of the nature and diagenesis of organic matter in the formation of petroleum. Am Assoc Pet Geol Bull 58:499–506
Totman Parrish J, Curtis RL (1982) Atmospheric circulation, upwelling, and organic rich rocks in the Mesozoic and Cenozoic eras. Palaeogeogr Palaeoclimatol Palaeoecol 40:31–66
Tsaparas N, Marcopoulou-Diacantoni A (2005) Tortonian scleractinian corals from the island of Gavdos (South Greece). Rev Paléobiol 24:629–637
Tserolas P, Maravelis AG, Pasadakis N, Zelilidis A (2018) Organic geochemical features of the Upper Miocene successions of Lefkas and Cephalonia islands, Ionian Sea, Greece: an integrated geochemical and statistical approach. Arab J Geosci 11:105. https ://doi.org/10.1007/s1251 7-018-3431-8
Tserolas P, Maravelis AG, Tsochandaris N, Pasadakis N, Zelilidis A (2019) Organic geochemistry of the Upper Miocene-Lower Pliocene sedimentary rocks in the Hellenic Fold and Thrust Belt, NW Corfu island, Ionian sea, NW Greece. Mar Pet Geol 106:17–29
Tsirambides A (2015) The unconventional hydrocarbon resources of Greece. Geol Q 59:479–490
Tyson RV (1995) Sedimentary organic matter: organic facies and palynofacies. Chapman & Hall, London
Vafidis A, Andronikidis A, Economou N, Panagopoulos G, Zelilidis A, Manoutsoglou E (2012) Reprocessing and interpretation of seismic reflection data at Messara Basin, Crete, Greece. J Balkan Geophys Soc 15(2):31–40
Van Baak CGC, Krijgsman W, Magyar I, Sztanó O, Golovina LA, Grothe A, Hoyle TM, Mandic O, Patina IS, Popov SV, Radionova EP, Stoica M, Vasiliev I (2017) Paratethys response to the Messinian salinity crisis. Earth-Sci Rev 172:193–223. https :// doi.org/10.1016/j.earsc irev.2017.07.015
Van der Zwaan GJ, Jorissen FJ (1991) Biofacial patterns in riverinduced shelf anoxia. Geol Soc Spec Publ 58:65–82
Van Hinsbergen DJJ, Hafkenscheid E, Spakman W, Meulenkamp JE, Wortel MJR (2005) Nappe stacking resulting from subduction of oceanic and continental lithosphere below Greece. Geology 33:325–328
Vandenbroucke M, Largeau C (2007) Kerogen origin, evolution and structure. Org Geochem 38:719–833
Vasiliev I, Karakitsios V, Bouloubassi I, Agiadi K, Kontakiotis G, Antonarakou A, Triantaphyllou M, Gogou A, Kafousia N, de Rafélis M, Zarkogiannis S, Kaczmar F, Parinos C, Pasadakis N (2019) Large sea surface temperature, salinity, and productivity-preservation changes preceding the onset of the Messinian Salinity Crisis in the Eastern Mediterranean Sea. Paleoceanogr Paleocl 34:182–202
Wandrey CJ (2006) Eocene to Miocene composite total petroleum system, Irrawadsy-Andaman and north Burma geologic provinces, Myanmar. In: Wandrey CJ (ed) Petroleum systems and related geologic studies in Region 8, South Asia. US, vol 2208-E. Geol. Surv. Bull., pp 1–26
Yang S, Schulz H-M (2019) Factors controlling the petroleum generation characteristics of Palaeogene source rocks in the Austrian Molasse Basin as revealed by principal component analysis biplots. Mar Petrol Geol 99:323–336

Zachariasse WJ, van Hinsbergen DJJ, Fortuin AR (2008) Mass wasting and uplift on Crete and Karpathos during the early Pliocene related to initiation of south Aegean left-lateral, strike-slip tectonics. GSA Bull 120:976–993

Zachariasse WJ, van Hinsbergen DJJ, Fortuin AR (2011) Formation and fragmentation of a late Miocene supradetachment basin in central Crete: implications for exhumation mechanisms of highpressure rocks in the Aegean forearc. Basin Res 23:678–701

Zelilidis A, Maravelis AG (2015) Introduction to the thematic issue: Adriatic and Ionian seas: proven petroleum systems and future prospects. J Pet Geol 38:247–254

Zelilidis A, Piper DJW, Vakalas I, Avramidis P, Getsos K (2003) Oil and gas plays in Albania: do equivalent plays exist in Greece? J Pet Geol 26:29–48

Zelilidis A, Maravelis AG, Tserolas P, Konstantopoulos PA (2015) An overview of the petroleum systems in the Ionian Zone, onshore NW Greece and Albania. J Pet Geol 38:331–348

Zelilidis A, Tserolas P, Chamilaki E, Pasadakis N, Kostopoulou S, Maravelis AG (2016) Hydrocarbon prospectivity in the Hellenic trench system: organic geochemistry and source rock potential of Upper Miocene-Lower Pliocene successions in the eastern Crete Island, Greece. Int J Earth Sci 105:1859–1878

Zhao XZ, Liu GD, Jin FM, Huang Z, Lu X, Sun M, Chen Z (2015) Distribution features and pattern of effective source rock in small faulted lacustrine basin: a case study of the Lower Cretaceous in Erlian Basin. Acta Pet Sin 36:641–652